DMD Fast Forward. Published on August 23, 2021 as DOI: 10.1124/dmd.121.000538
This article has not been copyedited and formatted. The final version may differ from this version.

Title Page

Successful Prediction of Human Fetal Exposure to P-gp Substrate Drugs Using the Proteomics-informed Relative Expression Factor Approach and PBPK Modeling and Simulation

Olena Anoshchenko, Flavia Storelli and Jashvant D. Unadkat

Department of Pharmaceutics, University of Washington, Seattle, WA

DMD Fast Forward. Published on August 23, 2021 as DOI: 10.1124/dmd.121.000538
This article has not been copyedited and formatted. The final version may differ from this version.

Running Title Page

Predicting Human Fetal Drug Exposure to P-gp Substrates

b) Corresponding author:

Dr. Jashvant D. Unadkat
Department of Pharmaceutics University of Washington
Box 357610
Seattle, WA 98195
Telephone: 206-543-9434
Fax: 206-543-3204
E-mail: jash@u.washington.edu

c) The number of text pages: 25

The number of tables: 1

The number of figures: 6

The number of references: 61

The number of words in the Abstract: 243

The number of words in Introduction: 807

The number of words in Discussion: 1905

d) Abbreviations used:

5^{th} percentile: 5^{th} percentile confidence value; 95^{th} percentile: 95^{th} percentile confidence value; AAFE: absolute average fold error; AUC_f: area under the curve of total fetal plasma concentration-time profile; AUC_m: area under the curve of total maternal plasma concentration-time profile; BCRP: breast cancer resistance protein; BID: *Bis in die*, twice daily; $CI_{90\%}$: 90% confidence interval spanning between 5th and 95th percentiles; $CL_{int,PD,placenta}$: intrinsic placental passive diffusion clearance; $CL_{int,Pgp,placenta}$: *In vivo* P-gp mediated efflux clearance from the placenta; C_{max}: maximum plasma drug concentration; C-T profile: drug plasma concentration-time profile; CYP: cytochrome P450; DEX: dexamethasone; DRV: darunavir; ER:

DMD Fast Forward. Published on August 23, 2021 as DOI: 10.1124/dmd.121.000538
This article has not been copyedited and formatted. The final version may differ from this version.

efflux ratio; ER-REF: efflux ratio-relative expression factor; fCL_{int}: fetal intrinsic hepatic clearance; $f_{t,P\text{-}gp}$: fraction of a drug transported by P-glycoprotein; $f_{u,f}$:unbound fractions in fetal plasma; $f_{u,m}$: unbound fractions in maternal plasma; GW: gestational week; hABCG2-MDCKII: Madin-Darby canine kidney cells II with overexpressed human ABCG2 [BCRP]; hMDR1-MDCK$^{cP\text{-}gp\ KO}$: Madin-Darby canine kidney II cells with overexpressed human multidrug resistance protein 1 [P-gp] and knocked out canine P-gp; IC_{50}: 50% of maximal inhibitory concentration; IV: intravenous; k_a: absorption rate constant; K_p: partition coefficient; $K_{p,uu}$: unbound partition coefficient; LC-MS/MS: liquid chromatography tandem mass spectrometry; LPV: lopinavir; LY: lucifer yellow; MDCK: Madin-Darby canine kidney; m-f PBPK model: maternal-fetal physiologically based pharmacokinetic model; MP: maternal plasma; P_{app}: apparent permeability; PIs: HIV protease inhibitors; PK: pharmacokinetic; PO: peroral; PopPK: population pharmacokinetic; PZS: prazosin; QD: *Quaque die*, once daily; QND: quinidine; REF: relative expression factor; RTV: ritonavir; SYT: syncytiotrophoblast; T_{lag}: lag time; TRQ: tariquidar; UV: Umbilical vein.

DMD Fast Forward. Published on August 23, 2021 as DOI: 10.1124/dmd.121.000538
This article has not been copyedited and formatted. The final version may differ from this version.

ABSTRACT

Many women take drugs during their pregnancy to treat a variety of clinical conditions. To optimize drug efficacy and reduce fetal toxicity, it is important to determine or predict fetal drug exposure throughout pregnancy. Previously, we developed and verified a maternal-fetal physiologically based pharmacokinetic (m-f PBPK) model to predict fetal $K_{p,uu}$ (unbound fetal plasma AUC/unbound maternal plasma AUC) of drugs that passively cross the placenta. Here, we used *in vitro* transport studies in Transwell®, in combination with our m-f PBPK model, to predict fetal $K_{p,uu}$ of drugs that are effluxed by placental P-glycoprotein (P-gp), namely dexamethasone, betamethasone, darunavir and lopinavir. Using Transwell®, we determined the efflux ratio (ER) of these drugs in hMDR1-MDCK$^{cP\text{-}gpKO}$ cells where human P-gp was overexpressed and the endogenous P-gp was knocked-out. Then, using the proteomics-informed efflux ratio-relative expressive factor (ER-REF) approach, we predicted the fetal $K_{p,uu}$ of these drugs at term. Finally, to verify our predictions, we compared them with the observed *in vivo* fetal $K_{p,uu}$ at term. The latter was estimated using our m-f PBPK model and published fetal (umbilical vein, UV)/maternal plasma drug concentrations obtained at term (UV/MP). Fetal $K_{p,uu}$ predictions for dexamethasone (0.63), betamethasone (0.59), darunavir (0.17) and lopinavir (0.08) were successful as they fell within the 90% confidence interval ($CI_{90\%}$) of the corresponding *in vivo* fetal $K_{p,uu}$ (0.30 – 0.66, 0.29 – 0.71, 0.11 – 0.22, 0.04 – 0.19, respectively). This is the first demonstration of successful prediction of fetal $K_{p,uu}$ of P-gp drug substrates from *in vitro* studies.

DMD Fast Forward. Published on August 23, 2021 as DOI: 10.1124/dmd.121.000538
This article has not been copyedited and formatted. The final version may differ from this version.

SIGNIFICANCE STATEMENT

For the first time, using *in vitro* studies in cells, we successfully predicted human fetal $K_{p,uu}$ of P-gp substrate drugs. This success confirms that our m-f PBPK model, combined with the ER-REF approach, can successfully predict fetal drug exposure to P-gp substrates. This success provides increased confidence in the use of the ER-REF approach, combined with our m-f PBPK model, to predict fetal $K_{p,uu}$ of drugs (transported by P-gp or other transporters), both at term and at earlier gestational ages.

DMD Fast Forward. Published on August 23, 2021 as DOI: 10.1124/dmd.121.000538
This article has not been copyedited and formatted. The final version may differ from this version.

INTRODUCTION (804/750 words)

More than half of all pregnant women take drugs (medication) throughout pregnancy and about 25% take drugs in the first trimester (Scaffidi, Mol, & Keelan, 2017). Drugs are administered either to treat the mother for various clinical conditions (e.g., depression, epilepsy, gestational diabetes) or to treat her fetus (e.g., to prevent poor lung development in case of preterm delivery or to prevent vertical transmission of HIV) (Sheffield et al., 2014). Despite the high frequency of drug use in pregnancy, little is known about the drug benefits and risks for the fetus, which are related to fetal drug exposure after maternal drug administration. Fetal drug exposure (defined as an area under drug plasma concentration-time profile, AUC) is determined by maternal drug exposure, placental transport/metabolism and fetal drug elimination (Zhang et al., 2017). The extent of fetal drug exposure can be evaluated by $K_{p,uu}$, the ratio of fetal to maternal unbound plasma AUCs after single or multiple dose drug administration or the corresponding average steady-state plasma concentrations (C_{ss}) after multiple dose administration (**Eq. 1**, where $f_{u,f}$ and $f_{u,m}$ are the fractions of unbound drug in fetal or maternal plasma, respectively).

$$K_{p,uu} = \frac{f_{u,f} \cdot AUC_f}{f_{u,m} \cdot AUC_m} = \frac{f_{u,f} \cdot C_{ss,f}}{f_{u,m} \cdot C_{ss,m}} \quad (1)$$

In the absence of placental transport (and feto-placental metabolism), fetal $K_{p,uu}$ is unity (i.e., drugs passively diffuse across the placenta from the mother to the fetus , yielding equal maternal and fetal unbound plasma AUCs). When placental drug efflux by transporters

DMD Fast Forward. Published on August 23, 2021 as DOI: 10.1124/dmd.121.000538
This article has not been copyedited and formatted. The final version may differ from this version.

abundant in the human placenta (e.g., by P-glycoprotein (P-gp) (Anoshchenko et al., 2020; Joshi et al., 2016; Mathias, Hitti, & Unadkat, 2005)) is present, $K_{p,uu}$ will be less than unity. Such placental drug efflux can modulate fetal exposure to drugs and, therefore, compromise efficacy (if the fetus is the therapeutic target) or reduce potential fetal toxicity.

In order to determine fetal $K_{p,uu}$ of a drug at any gestational age, measurement of fetal (and maternal) drug plasma concentrations is necessary. However, except at term, for ethical and logistical reasons, it is impossible to measure fetal (e.g., umbilical vein) drug concentrations. Various *in vitro* systems have attempted to mimic the syncytiotrophoblast (SYT) placental barrier that could aid in $K_{p,uu}$ estimation (Arumugasaamy, Rock, Kuo, Bale, & Fisher, 2020), but most of them fail to recapitulate the complexity of SYT layer *in vivo* (e.g., BeWo, JAR, Jeg-3 cell monolayers), are laborious (perfused human placenta) or at very early stages of development (microphysiological systems). Due to the limitations of the aforementioned systems and the lack of clinical data at earlier gestational ages, an alternative is to **predict**, as opposed to **measure**, fetal $K_{p,uu}$. Such predictions can be made and verified at term using physiologically-based pharmacokinetic (PBPK) modeling and simulation (M&S).

We have previously developed and verified a maternal-fetal PBPK (m-f PBPK) model capable of predicting maternal-fetal exposure to drugs that are metabolized by various CYP enzymes (Ke, Nallani, Zhao, Rostami-Hodjegan, & Unadkat, 2012, 2014) and cross the placenta by passive diffusion (Zhang et al., 2017; Zhang & Unadkat, 2017). However, many drugs administered to pregnant women are substrates of efflux transporters that are highly expressed in the placenta such as P-glycoprotein (P-gp) and Breast Cancer Resistance Protein (BCRP) (Anoshchenko et al., 2020; Mathias et al., 2005). Both serve to reduce fetal exposure to drugs such as

DMD Fast Forward. Published on August 23, 2021 as DOI: 10.1124/dmd.121.000538
This article has not been copyedited and formatted. The final version may differ from this version.

corticosteroids (Petersen, Nation, Ashley, & McBride, 1980; Tsuei, Petersen, Ashley, McBride, & Moore, 1980), HIV protease inhibitors (Colbers, Greupink, Litjens, Burger, & Russel, 2016; Fauchet et al., 2015) or anti-cancer drugs (e.g., imatinib)(Russell, Carpenter, Akhtar, Lagattuta, & Egorin, 2007). Therefore, to make our m-f PBPK model comprehensive, we combined it with the efflux ratio-relative expression factor approach (ER-REF) to predict fetal $K_{p,uu}$ of drugs that are actively transported by the placenta. The ER-REF approach to predict $K_{p,uu}$ has been described previously to predict brain distribution of transporter substrates in humans and preclinical species (Storelli, Anoshchenko, & Unadkat, 2021; Trapa et al., 2019; Uchida, Ohtsuki, Kamiie, & Terasaki, 2011; Uchida et al., 2014). It relies on measurement of 1) transport clearance of the drugs (i.e., via the efflux ratio, ER) in transporter-overexpressing cell lines (e.g., Transwell®) and 2) transporter abundance in both *in vivo* tissue (the placenta) and transporter-overexpressing cell lines using quantitative targeted proteomics to obtain REF (see, **Figure 1** for workflow).

Using this efflux ratio-relative expression factor approach (ER-REF), combined with our m-f PBPK model, we predicted the fetal $K_{p,uu}$, of four model P-gp substrate drugs, namely two antenatal corticosteroids (ACS), dexamethasone (DEX) and betamethasone (BET) and two HIV protease inhibitors (PIs), darunavir (DRV) and lopinavir (LPV). Then, to verify our $K_{p,uu}$ predictions we compared these predictions with the corresponding estimated *in vivo* fetal $K_{p,uu}$ of these drugs. The latter was estimated from m-f PBPK modeling of the observed maternal and fetal (umbilical vein) plasma concentrations of these drugs, obtained at term (or close to term), in a number of maternal-fetal dyads (**Figure 1**).

DMD Fast Forward. Published on August 23, 2021 as DOI: 10.1124/dmd.121.000538
This article has not been copyedited and formatted. The final version may differ from this version.

METHOD

Chemicals and Reagents for Transport Assays.

See **Supplementary Information.**

Cell Culture for Transwell Transport Assays

Human P-gp overexpressing MDCKII cells where the endogenous canine P-gp was knocked-out (hMDR1-MDCK$^{cP\text{-}gpKO}$), were generously provided by Dr. Per Artursson, Uppsala University. hMDR1-MDCK$^{cP\text{-}gpKO}$ cells were cultured in high-glucose DMEM that contained 10% FBS, 1% penicillin (10,000 U/mL)/streptomycin (10,000 g/mL), 2mM Glutamax^{TM} and 375 µg/mL Hygromycin B. The human BCRP-overexpressing MDCKII (hABCG2-MDCKII) cells, generously provided by Dr Qingcheng Mao, University of Washington, were cultured in low-glucose DMEM that contained 10% FBS, 1% penicillin (10,000 U/mL)/streptomycin (10,000 g/mL) and 500 µg/mL geneticin. Cells were grown at 37°C, 5% CO_2, and 95% humidity, harvested using trypsin and subcultured twice a week.

Transwell Transport Assay

The efflux ration (ER) of DEX, BET, DRV (2 µM each), LPV (0.4 µM [^{3}H]LPV + 0.6 µM LPV) was determined in four independent experiments (each conducted in triplicate) in hMDR1-MDCK$^{cP\text{-}gpKO}$ cells. ER of DEX, BET (2 µM each) was also determined in four independent experiments (each conducted in triplicate) in hABCG2-MDCKII cells. Quinidine (QND, 3 µM), prazosin (PZS, 3 µM) and lucifer yellow (LY) were included in the above determinations as markers of robust P-

DMD Fast Forward. Published on August 23, 2021 as DOI: 10.1124/dmd.121.000538
This article has not been copyedited and formatted. The final version may differ from this version.

gp, BCRP activity and integrity of tight junction, respectively. ER was estimated by conducting each experiment in two directions: A→B where the donor was the apical (A) compartment (volume = 0.5 mL) and the receiver (B) was the basal compartment (volume = 1 mL) or vice versa, B→A.

Briefly, on day 0, 6 x 10^5 cells/well were plated on apical side of the 12-well Transwell® polyester insert. Cells were grown in plates for 4 days prior to experiment with the change of medium on day 2. Medium was changed on day 2 and 3. On day 4, cells were washed 3 times with 37°C transport buffer (10 mM HEPES in HBSS at pH 7.4) and incubated in an orbital shaker at 120 rpm. The donor solution ± tariquidar 5 µM (P-gp inhibitor in hMDR1-MDCK$^{cP\text{-}gpKO}$ cells) or ± Ko143 5 µM (BCRP inhibitor in hABCG2-MDCKII cells) was prepared in transport buffer containing the drug and 50 µM paracellular transport marker lucifer yellow (LY). The receiver solution contained transport buffer ± tariquidar (5 µM) or ± Ko143 (5 µM). Transport assay was initiated by adding the donor solution to the donor compartment and performed at 37°C with 120 rpm shaking. Donor compartments were sampled (10 µL) at time 0 and at the end of the transport experiment. Receiver compartments were sampled (100 µL) at 15, 30, 45 and 60 min (DEX, BET); 7, 15, 30, 45 min (DRV); 60, 120, 180 and 240 min (LPV) and replenished with the incubation medium. At the end of each experiment cells were washed 3 times with ice-cold transport buffer and lysed for drug or marker assay, total protein content (BCA) and proteomic analysis.

DMD Fast Forward. Published on August 23, 2021 as DOI: 10.1124/dmd.121.000538
This article has not been copyedited and formatted. The final version may differ from this version.

Quantification of Drugs and Markers

[^{3}H]LPV was quantified using scintillation counting (PerkinElmer, Waltham, MA). DEX, BET, DRV, QND and PZS were quantified using liquid chromatography-tandem mass spectrometry (LC-MS/MS) on AB Sciex Triple Quad 6500 (SCIEX, Farmingham, MA) instrument coupled with Waters Acquity UPLC system (Waters, Hertfordshire, UK). Briefly, 100 µL of acetonitrile containing 0.5 nM N-desmethyl loperamide as internal standard (IS) were added to 50 µL of donor/receiver samples in 96-well plates. Samples were centrifuged at 3220 g, 4°C for 15 min and the supernatant was injected into the LC-MS/MS (see **Tables S1 and S2** for details on LC-MS/MS method and chromatographic conditions). All drug concentrations (diluted where necessary) fell within the linear range of peak area ratios with a signal-to-noise ratio of >5. The permeability of the paracellular marker lucifer yellow (LY) was analyzed on Synergy HTX fluorescence reader (Biotek, Winooski, VT, USA) with excitation/emission wavelength 480/530 nm. The linearity of LC-MS/MS signal (in peak area units) and fluorescence reader signal (in relative fluorescent units) within the quantified work range, was confirmed by preliminary experiments (data not shown).

Determination of *in vitro* Efflux Ratios (ER)

ER in the absence and presence of P-gp or BCRP inhibitors were determined in the *in vitro* Transwell® assay (**Eq 2**),

$$ER = \frac{P_{app(B\rightarrow A)}}{P_{app(A\rightarrow B)}} = \frac{CL_{int(B\rightarrow A)}}{CL_{int(A\rightarrow B)}} = \frac{cA_{A(R)} \cdot AUC_{A(D)}}{AUC_{B(D)} \cdot cA_{B(R)}} \qquad (2)$$

DMD Fast Forward. Published on August 23, 2021 as DOI: 10.1124/dmd.121.000538
This article has not been copyedited and formatted. The final version may differ from this version.

where $P_{app(B\rightarrow A)}$ and $P_{app(A\rightarrow B)}$ are apparent permeabilities and since the surface area is identical in both direction these are equivalent to $CL_{int(B\rightarrow A)}$ and $CL_{int(A\rightarrow B)}$, the apparent intrinsic clearances of a drug in indicated directions; $cA_{A(R)}$ and $cA_{B(R)}$ are cumulative amounts of drug in corresponding receiver compartment, $AUC_{A(D)}$ and $AUC_{B(D)}$ are AUC of the drug in corresponding donor compartment. $cA_{A(R)}$ and $cA_{B(R)}$ were corrected for the sampled volume at each time point. We used $AUC_{A(D)}$ and $AUC_{B(D)}$ instead of single donor drug concentration at time 0, because this approach corrects for the depletion of the drug in the donor compartment during the experiment. Only experiments with integral tight junctions (LY apparent permeability - P_{app} < $2\cdot10^{-6}$ cm/s) were used for further analyses. Likewise, only experiments with ER >7 for QND or PRZ were included in our analyses. Grouped statistical analysis of ER and P_{app} values was performed by Kruskal-Wallis with Dunn's multiple comparisons test, $p<0.05$.

Prediction of fetal $K_{p,uu}$ from *in vitro* studies using the ER-REF approach

The *in vivo* $K_{p,uu}$ is related to the clearances mediating the entry and exit of the unbound drug into and from the fetal compartment, respectively, provided fetal elimination of the drug is negligible (see later for justification of this assumption) (**Eq. 3**).

$$K_{p,uu} = \frac{CL_{\text{int,PD,placenta}}}{CL_{\text{int,PD,placenta}} + CL_{\text{int,P-gp,placenta}}} \quad (3)$$

Dividing by $CL_{int,PD,\ placenta}$ yields:

$$K_{p,uu} = \frac{1}{1 + \frac{CL_{int,P-gp,placenta}}{CL_{int,PD,placenta}}} \quad (4)$$

DMD Fast Forward. Published on August 23, 2021 as DOI: 10.1124/dmd.121.000538
This article has not been copyedited and formatted. The final version may differ from this version.

Therefore, the *in vivo* $K_{p,uu}$ (**Eq. 4**) can be related to the *in vitro* P-gp mediated ER as follows:

$$K_{p,uu} = \frac{1}{1+\left(ER_{TRQ(-)} - ER_{TRQ(+)}\right)\cdot REF} \quad (5)$$

where the ER in the presence and absence of TRQ is the P-gp mediated ER. To scale this P-gp mediated ER to that *in vivo*, the difference in the abundance of P-gp between *in vitro* (i.e., hMDR1-MDCK$^{cP\text{-}gpKO}$ cells) and *in vivo* should be accounted for. The relative expression factor (REF) corrects for this difference in abundance. P-gp abundance in cells and *in vivo* in human placentae was quantified as described below and before (Anoshchenko et al., 2020), respectively.

$$REF = \frac{P-gp\ abundance\ in\ human\ placenta\ (pmol/mg\ HP)}{P-gp\ abundance\ in\ hMDR1-MDCKII^{cP-gp\ KO}\ cell\ line\ (pmol/mg\ HP)} \quad (6)$$

where HP is the total protein in the homogenate of the human placenta or hMDR1-MDCK$^{cP\text{-}gpKO}$ cells.

Based on the above equations, when a drug is not a substrate of P-gp and/or BCRP, $K_{p,uu}$ and ER will both equal 1. When a drug is actively effluxed, $K_{p,uu}$ will be <1 and ER>1. The fraction of a drug transported by P-gp ($f_{t,P\text{-}gp}$) was then calculated from predicted $K_{p,uu}$ value of each drug ($f_{t,P\text{-}gp} = 1 - K_{p,uu}$).

DMD Fast Forward. Published on August 23, 2021 as DOI: 10.1124/dmd.121.000538
This article has not been copyedited and formatted. The final version may differ from this version.

Quantification of P-gp Abundance in hMDR1-MDCK$^{cP\text{-}gpKO}$ Cells and Determination of the relative expression factor (REF)

After each experiment, cells were lysed on the semi-permeable membranes in 1:1 ratio of 2%SDS:EBII buffer for 60 min at room temperature, total protein concentration was measured by BCA assay and approximately 110-160 µg of total protein were reduced, alkylated and trypsin digested in duplicates as described before (Anoshchenko et al., 2020; Billington et al., 2019; Storelli, Billington, Kumar, & Unadkat, 2020). Ice-cold heavy-labeled IS peptide (NTTGALTTR) was prepared in 80% acetonitrile plus 0.2% formic acid solution and spiked into the trypsin digest (in 1:4 IS : sample ratio) to terminate trypsin digestion. After centrifugation (5000g, 4°C), 5 µL of supernatant were injected onto the LC-MS/MS system and analyzed using settings and procedure described before (Anoshchenko et al., 2020). Pooled human placental total membrane sample was used as biological control and digested with experimental samples. Calibration curve (0.62 – 40 nM) and quality control samples (0.62, 10, 40 nM) were prepared in 50 mM ammonium bicarbonate buffer, 10 ul of unlabeled peptide standard and 20 µl of chilled labeled peptide internal standard (both in 80% acetonitrile and 0.2% formic acid solution). P-gp abundance in the homogenate of the term placenta (0.16 ± 0.07 pmol/mg of homogenate protein, (Anoshchenko et al., 2020)) was used to estimate the REF value (**Eq. 6**).

Estimation of Fetal $K_{p,uu}$ Using the Observed *in vivo* Data

Fetal *in vivo* $K_{p,uu}$ of DRV and LPV was estimated as we have previously described for DEX and BET (**manuscript in press**). DRV and LPV are usually administered in combination with ritonavir (RTV). The observed DRV and LPV data in non-pregnant and pregnant women (including UV

DMD Fast Forward. Published on August 23, 2021 as DOI: 10.1124/dmd.121.000538
This article has not been copyedited and formatted. The final version may differ from this version.

plasma concentrations) are available only for the combination drug dosing regimens, DRV/RTV or LPV/RTV. As an overview (see below for details), we first optimized SimCYP® PBPK model of DRV/RTV and LPV/RTV in non-pregnant individuals after oral (PO) drug administration of each combination drug regimen. To do so, the model was populated with physicochemical and pharmacokinetic parameters for DRV, LPV and RTV (Wagner et al., 2017) and verified using the observed drug plasma concentration-time profiles (C-T profiles) in the non-pregnant population (Boffito, Miralles, & Hill, 2008; Eron et al., 2004; V. Sekar et al., 2010; V. J. Sekar, Lefebvre, De Pauw, Vangeneugden, & Hoetelmans, 2008). Then, the parameters from non-pregnant population were incorporated into m-f PBPK model and adjusted for pregnancy-induced physiological changes (e.g., placental and hepatic blood flow, hepatic CYP3A induction, etc.) at the gestational week (average demographic) specified in the observed data sets. Finally, fetal-placental clearance parameters of DRV and LPV were optimized to estimate the *in vivo* fetal $K_{p,uu}$.

I. Optimization of PBPK Models of DRV and LPV in the Non-pregnant Population

We first predicted plasma concentration-time (C-T) profiles of DRV administered alone (PO 400 mg BID, data not shown), DRV/RTV (PO 600/100 mg BID and 800/100 mg QD) and LPV/RTV (PO 400/100 mg BID) in the non-pregnant population using SimCYP Simulator® Version 19 (SimCYP Ltd., A Certara Company, Sheffield, UK). The previously published DRV, LPV, RTV drug-specific parameters were used (Wagner et al., 2017) except that some of them (t_{lag}, k_a) were optimized (DRV: t_{lag} = 1.3 h, k_a = 0.4 h^{-1} and LPV: t_{lag} = 1.5 h) until the predicted steady-state DRV or LPV plasma concentration data adequately described the observed data. The observed DRV or LPV steady-state C-T data (Boffito et al., 2008; Eron et al., 2004; V. Sekar et al., 2010; V. J. Sekar et

DMD Fast Forward. Published on August 23, 2021 as DOI: 10.1124/dmd.121.000538
This article has not been copyedited and formatted. The final version may differ from this version.

al., 2008) were digitized with WebPlotDigitizer (https://automeris.io/WebPlotDigitizer/). RTV drug-specific parameters included the time-dependent inactivation and induction of CYP3A enzymes in the intestine and the liver.

II. Verification of the m-f PBPK Models of DRV (at gestational week - GW34 and GW38) and LPV (GW 38) in the Pregnant Population.

CYP3A inhibition by RTV in pregnancy was first generated in the SimCYP® pregnancy model. Then, the change in bioavailability of DRV or LPV in pregnancy, due to co-administration of RTV, (13-fold for DRV and 112-fold for LPV) was incorporated into our m-f PBPK model based on the values determined in SimCYP pregnancy model at the corresponding gestational age. The DRV and LPV steady-state PK parameters obtained in non-pregnant population were incorporated into our m-f PBPK model built in MATLAB R2020a using our previously published approach (manuscript in press). As per our previous publications, compared to non-pregnant individuals, we assumed maternal hepatic CYP3A activity was induced at term by 2-fold (Hebert et al., 2008; Zhang, Farooq, Prasad, Grepper, & Unadkat, 2015). For DRV two sets of maternal C-T profile predictions were generated due to the presence of intensively-sampled observed data at GW34 and sparsely sampled data at GW38 (latter, with matching sparsely-sampled fetal UV data).

III. Optimization of Fetal-Placental PK parameters of DRV and LPV at gestational week 38 (GW38) to estimate in vivo fetal $K_{p,uu}$

As described before (Zhang & Unadkat, 2017), we estimated the *in vivo* transplacental passive diffusion clearance ($CL_{int,PD,placenta}$) of DRV and LPV by scaling the *in vivo* midazolam $CL_{int,PD,placenta}$ by the ratio of the apparent permeabilities (P_{app}'s) of the two drugs in hMDR1-MDCK$^{cP\text{-}gpKO}$ cells (1.19×10^{-5} and $1.25\ \ 10^{-5}$ cm/s, respectively) and that of midazolam (MDZ $CL_{int,PD,placenta}$

DMD Fast Forward. Published on August 23, 2021 as DOI: 10.1124/dmd.121.000538
This article has not been copyedited and formatted. The final version may differ from this version.

=500L/h, P_{app} =4.9 x 10^{-5} cm/s; determined in MDCKII or Caco-2 cells). The resulting DRV and LPV $CL_{int,PD,placenta}$ were 121 and 127 L/h, respectively, values that were much greater than the placental blood flow at term (~45 L/h). Therefore, DRV and LPV $CL_{int,PD,placenta}$ were considered to be perfusion-limited (45 L/h). Fetal hepatic intrinsic clearance (fCL_{int}) was assumed to be negligible due to low CYP3A7 turnover of CYP3A metabolized drugs and low fetal liver weight (Zhang & Unadkat, 2017)(manuscript in press). Then, as we have described before (manuscript in press), the *in vivo* fetal $K_{p,uu}$ value was optimized by adjusting $CL_{int,P\text{-}gp,placenta}$ until the predicted unbound UV/MP best described the observed unbound UV/MP (by minimizing the absolute average fold error, AAFE). The observed maternal and UV steady-state C-T profiles of DRV were obtained from published literature (Colbers et al., 2015; Murtagh et al., 2019; Stek et al., 2015). These C-T profiles were digitized with WebPlotDigitizer (https://automeris.io/WebPlotDigitizer/). Because the observed C-T profiles of LPV (Cressey et al., 2015; Fauchet et al., 2015) were highly variable, we used the UV and MP C-T profiles predicted by a population pharmacokinetic (PopPK) model that was previously fitted by others to the UV and MP LPV C-T profiles (Cressey et al., 2015; Fauchet et al., 2015). To generate interindividual variability in the plasma C-T profiles, a virtual population of 100 individuals was simulated within m-f PBPK model to generate the mean, 5^{th} and the 95^{th} percentile profiles (90% confidence interval – $CI_{90\%}$).

DMD Fast Forward. Published on August 23, 2021 as DOI: 10.1124/dmd.121.000538
This article has not been copyedited and formatted. The final version may differ from this version.

Prediction of DRV and LPV Pharmacokinetics in the Pregnant Population at an Earlier Gestational Age (Week 20; GW20)

To illustrate the utility of our model to predict fetal exposure to drugs at earlier gestational age, we predicted the DRV and LPV maternal-fetal profiles at gestational week 20 (GW20). GW20 was chosen since this is the earliest gestational age at which all the fetal physiological parameters (e.g., organ volumes, partition coefficients, blood flows) are available. First, the m-f PBPK model was populated with both maternal and fetal physiological and hepatic CYP3A activity applicable to GW20 using the gestational age-dependent changes in the parameters that we have published previously (Zhang et al., 2015; Zhang et al., 2017). Then, $CL_{int,PD,placenta}$ and $CL_{int,P\text{-}gp,placenta}$ (at GW20) for both drugs were adjusted for the GW20 placental surface area (Zhang et al., 2017) and total placental P-gp abundance we have previously quantified (Anoshchenko et al., 2020). Finally, GW20 maternal and fetal C-T profiles at steady-state (dose 16) were generated after PO DRV/RTV 600/100 BID and PO LPV/RTV 400/100 BID.

Statistical Analyses and Verification of Predictions

Our acceptance criteria for non-pregnant PBPK and m-f PBPK model verifications were to predict pharmacokinetic parameters (C_{max}, AUC and CL) within 0.8 – 1.25-fold of the observed values and absolute average fold error (AAFE, where available) of <2. Interindividual variability and $CI_{90\%}$ (5^{th} and 95^{th} percentiles) for C-T profiles and $K_{p,uu}$ were generated in a virtual population of 100 individuals and included variability only in the maternal system-related parameters. The 90% confidence interval ($CI_{90\%}$) of the predicted fetal $K_{p,uu}$ was generated using pooled variance approach (O'Neill., 2014), where the variability in ER and REF (P-gp

DMD Fast Forward. Published on August 23, 2021 as DOI: 10.1124/dmd.121.000538
This article has not been copyedited and formatted. The final version may differ from this version.

abundances *in vitro* cell line and *in vivo* placental tissue) were included. Verification of the predicted fetal $K_{p,uu}$ (using the ER-REF approach) was deemed successful if the mean predicted fetal $K_{p,uu}$ fell within $CI_{90\%}$ of the observed fetal $K_{p,uu}$.

DMD Fast Forward. Published on August 23, 2021 as DOI: 10.1124/dmd.121.000538
This article has not been copyedited and formatted. The final version may differ from this version.

RESULT

ER of DEX, BET, DRV and LPV in Transwell assays using hMDR1-MDCK$^{cP\text{-}gp\ KO}$ or hABCG2-MDCKII cells

DEX, BET, DRV and LPV were transported by P-gp as evidenced by their P-gp mediated efflux ratios ($ER_{P\text{-}gp}$) in hMDR1-MDCK$^{cP\text{-}gp\ KO}$ cells (**Figure 2, Table 1**). In the same experiments, the ER of the positive control quinidine (QND) was 11.1 ± 2.5 (mean ± SD, n=4 experiments, each conducted in triplicate, data not shown). In contrast, DEX and BET were not transported by BCRP. Their ER in hABCG2-MDCKII cells was 1.2 ± 0.3 and 1.1 ± 0.1, respectively (**Figure 2C**). In the same experiments, the ER of the BCRP positive-control substrate prazosin (PZS), was 7.1 ± 2.5 (mean ± SD, n=4 experiments, each conducted in triplicate, data not shown). The HIV PIs were not tested in hABCG2-MDCKII cells as published data indicate that they do not appear to be BCRP substrates (Agarwal, Pal, & Mitra, 2007; Konig et al., 2010).

Estimates of *in vivo* Fetal $K_{p,uu}$ Obtained Using our m-f PBPK Model

To estimate the *in vivo* fetal $K_{p,uu}$ (to verify our ER-REF predictions) we first successfully predicted C-T profiles and pharmacokinetic parameters of LPV and DRV in the non-pregnant population after PO DRV/RTV 600/100 BID (**Figure 3 A1, A2),** DRV/RTV PO 800/100 QD (**Figure S3 A1, A2)** or LPV/RTV PO 400/100 BID (**Figure 4 A1, A2**). Then, using our m-f PBPK model (which incorporates pregnancy-induced changes in pharmacokinetic and physiological parameters at gestational week (average demographic) specified in observed data sets, we predicted the C-T profiles of LPV (GW38: **Figure 4 B1**) or DRV (GW34: **Figure 3 B1**; GW38 **Figure**

DMD Fast Forward. Published on August 23, 2021 as DOI: 10.1124/dmd.121.000538
This article has not been copyedited and formatted. The final version may differ from this version.

3 C1) in pregnant women who were administered the above dosing regimens. The predicted C-T profiles in pregnant women were successfully verified as evidenced by comparing the predicted and observed data (**Figure 3 B1** and **4 B1**: predicted $CI_{90\%}$ captured observed/PopPK predicted data; **Figure 3 C1**: AAFE = 1.93 and **Figure S3 C1**: AAFE = 1.72) and the predicted pharmacokinetic parameters falling within 0.8 and 1.25-fold of the observed data (our predefined acceptance criteria) (**Figure 3 B2**; **Figure S3 B2** and **Figure 4 B2,** respectively).

Once the maternal C-T profiles were verified, we optimized the *in vivo* placental P-gp mediated efflux clearance ($CL_{int,P\text{-}gp,placenta}$) for DRV and LPV using our m-f PBPK model and published UV/MP data at term (**Figure 3, 4**). For DRV, *in vivo* placental efflux clearance ($CL_{int,P\text{-}gp,placenta}$=612 L/h), yielding $K_{p,uu}$ = 0.16, resulted in the best prediction of UV/MP ratio (AAFE=1.63) compared with when no $CL_{int,P\text{-}gp,placenta}$ was invoked (AAFE=8.35, $K_{p,uu}$=1) (**Figure 3 E1, E2**). For LPV, *in vivo* placental efflux clearance ($CL_{int,P\text{-}gp,placenta}$=1029 L/h) yielding $K_{p,uu}$ = 0.11 resulted in the best prediction of UV/MP ratio (AAFE=1.17) compared to when no $CL_{int,P\text{-}gp,placenta}$ was invoked (AAFE=6.42, $K_{p,uu}$=1) (**Figure 4 D1, D2**). DEX and BET *in vivo* $K_{p,uu}$ were similarly estimated (0.48 and 0.5, respectively) and obtained from our submitted publication.

Prediction and verification of fetal $K_{p,uu}$ using the ER-REF approach

After the *in vitro* ER of DEX, BET, DRV and LPV, were scaled using the ER-REF approach (**Eq. 5, 6**), the predicted *in vivo* fetal $K_{p,uu}$ (mean and $CI_{90\%}$) obtained were 0.63 (0.48 – 0.78), 0.59 (0.42 – 0.69), 0.17 (0.1 – 0.23), 0.08 (0.07 – 0.1) respectively (**Figure 5 Table 1**). The mean ER-REF predicted values fell within $CI_{90\%}$ of estimated from *in vivo* values for DEX (0.3 – 0.66), BET (0.29

DMD Fast Forward. Published on August 23, 2021 as DOI: 10.1124/dmd.121.000538
This article has not been copyedited and formatted. The final version may differ from this version.

– 0.71), DRV (0.11 – 0.22) and LPV (0.04 – 0.19), demonstrating success of the ER-REF approach (**Figure 5, Table 1**). These mean ER-REF predicted $K_{p,uu}$ resulted in UV/MP ratio profiles that predicted the observed values well described (DRV, LPV **Figure S4 A, B**) or modestly overpredicted the observed values (BET, DEX **Figure S4 C, D**). These ER-REF predicted $K_{p,uu}$ values yielded mean *in vivo* fraction of drug transported by placental P-gp ($f_{t,P\text{-}gp} = 1 - K_{p,uu}$) of 0.37, 0.41, 0.84 and 0.92 for DEX, BET, DRV and LPV, respectively.

Prediction of DRV/RTV and LPV/RTV $K_{p,uu}$ at an earlier gestational age (GW20)

At GW20, $CL_{int,PD,placenta}$ for DRV and LPV were 47 and 49.5 L/h, respectively (calculated from term $CL_{int,PD,placenta}$ values by adjusting for the change in placental surface area between two gestational ages). These values exceeded placental blood flow at this gestational age (27.5 L/h), yielding perfusion-limited $CL_{int,PD,placenta}$. $CL_{int,P\text{-}gp,placenta}$ at GW20, adjusted for decrease in total placental P-gp abundance at this gestational age (Anoshchenko et al., 2020), resulted in values 40% lower than the corresponding values at GW38 (367 and 617 L/h for DRV and LPV, respectively). After gestational-age adjustment of other maternal-fetal physiological and pharmacokinetic parameters, the m-f PBPK model predicted fetal DRV and LPV UV plasma AUCs were respectively 43% and 38% of that at GW38. In contrast, the corresponding maternal plasma AUC of DRV was unchanged while that of LPV was modestly, 1.15-fold, higher at GW20 than at GW38 (**Figure 6**). These changes predicted DRV and LPV fetal $K_{p,uu}$'s at GW20 of 0.11 and 0.07, respectively (69% and 64% of that at GW38)

DMD Fast Forward. Published on August 23, 2021 as DOI: 10.1124/dmd.121.000538
This article has not been copyedited and formatted. The final version may differ from this version.

DISCUSSION

Using our m-f PBPK model, we have successfully predicted and verified fetal exposure to drugs that passively cross the placenta (Zhang & Unadkat, 2017). However, pregnant women often take drugs that are effluxed by placental transporters. We have previously shown that REF approach can successfully predict transporter-based clearance and tissues concentration of drugs (Ishida, Ullah, Toth, Juhasz, & Unadkat, 2018; A. R. Kumar et al., 2021; V. Kumar et al., 2018; Sachar, Kumar, Gormsen, Munk, & Unadkat, 2020; Storelli et al., 2021). Similarly, here we determined if our ER-REF approach, combined with our m-f PBPK model, could predict fetal exposure to drugs that are transported by placental transporters. We chose to test this hypothesis using the placental P-gp transporter as our model transporter because, of all the transporters expressed in the placenta, it is arguably the most important in modulating fetal drug distribution. This is because it is highly abundant in the human placentae (Anoshchenko et al., 2020; Joshi et al., 2016; Mathias et al., 2005) and is capable of transporting wide variety of marketed drugs (Schinkel & Jonker, 2003). Indeed, many drugs (e.g., antibiotics, cardiac drugs, antiemetics, HIV drugs) taken by pregnant women are effluxed by placental P-gp. Here, using the ER-REF approach, combined with our m-f PBPK model, we present the first successful prediction of fetal $K_{p,uu}$, at term, for drugs that are transported by the human placentae. Moreover, our predicted fetal $K_{p,uu}$ were verified by data observed at term. Although we would have preferred to conduct verification of our prediction at several gestational ages, such verification is not possible due to unavailability of UV and MP data at gestational ages other than term.

DMD Fast Forward. Published on August 23, 2021 as DOI: 10.1124/dmd.121.000538
This article has not been copyedited and formatted. The final version may differ from this version.

Our ER-REF approach deliberately incorporated several elements to enhance our success in $K_{p,uu}$ predictions. First, we used transfected MDCK cell line that had the endogenous canine P-gp knocked out. Therefore, our measured ER and predicted fetal $K_{p,uu}$ were not confounded by endogenous canine P-gp activity. Second, we measured P-gp abundance in hMDR1-MDCK$^{cP\text{-}gpKO}$ cells in each independent transport experiment and, hence, our REF was not confounded by differences in *in vitro* transporter abundance between cell passage numbers (**Table 1**). Third, the quantification of P-gp abundance *in vitro* was performed using the same method as for *in vivo* placental tissue (Anoshchenko et al., 2020), within the same lab, hence minimizing bias (due to interlaboratory variability in proteomics quantification) in determining REF. Fourth, we chose to study drugs that were selective for a given transporter, namely P-glycoprotein. Thus, the presence of other transporters in the placenta (e.g., BCRP) did not confound the observed or predicted *in vivo* fetal $K_{p,uu}$. Indeed, we showed that the ACS were not substrates of BCRP (ER<2 in hABCG2-MDCKII cells – **Figure 2C**). And, literature data suggest that the PIs, DRV and LPV, are also unlikely substrates of BCRP (Agarwal et al., 2007; Konig et al., 2010). Fifth, none of the drugs are likely to be significantly metabolized in placenta which would also confound interpretation of the *in vivo* $K_{p,uu}$. All four drugs are primarily metabolized by CYP3A, the enzyme with relatively low placental abundance and activity (Myllynen, Immonen, Kummu, & Vahakangas, 2009; Myllynen, Pasanen, & Vahakangas, 2007; Pasanen, 1999). Besides CYP3A, DEX and BET can also be metabolized by 11 β-hydroxysteroid dehydrogenase-2 enzyme present in placenta, although the rate and extent of such metabolism relative to $CL_{int,PD,placenta}$ and $CL_{int,P\text{-}gp,placenta}$ is low (e.g., ~10-15% of DEX/BET metabolized over 6 h *in vitro* in placental microsomes)(Blanford & Murphy, 1977; Murphy et al., 2007). Sixth, we confirmed that the ER

DMD Fast Forward. Published on August 23, 2021 as DOI: 10.1124/dmd.121.000538
This article has not been copyedited and formatted. The final version may differ from this version.

of the ACS drugs in our Transwell assays was independent of concentration (over the range 2 - 250 µM). Due to low solubility of DRV and LPV (16 and 3 µM, respectively - DrugBank database), a similar study over a wide range of concentrations was not feasible. Therefore, for our Transwell assays we selected the lowest concentration of all four drugs that was quantifiable by our analytical method (2 µM for DEX/BET/DRV and 1 µM for LPV). Although RTV has been reported to be a P-gp inhibitor, based on the reported *in vivo* plasma concentration of the drug at the doses administered together with DRV or LPV, it is highly unlikely to inhibit placental P-gp *in vivo*. The highest reported maternal plasma RTV unbound C_{max} is 13 nM (Stek et al., 2015) (at 100 mg, BID), much lower than the lowest reported RTV IC_{50} for P-gp (240 nM, (Vermeer, Isringhausen, Ogilvie, & Buckley, 2016). Additionally*, in vivo* data (Gimenez, Fernandez, & Mabondzo, 2004) also supports that low-dose RTV is unlikely to inhibit brain P-gp in human (Tayrouz et al., 2001) or mice (Gimenez et al., 2004; Huisman et al., 2001). Therefore, in determining DRV or LPV ER in hMDR1-MDCK$^{cP\text{-}gp\ KO}$ cells, RTV was not added to the donor compartment. Seventh, interestingly, although the *in vivo* $K_{p,uu}$ of the PIs was estimated from data obtained when they were co-administered with RTV (a potent intestinal CYP3A inhibitor), incorporating 2-fold induction of hepatic CYP3A4 in pregnancy (Hebert et al., 2008) into the m-f PBPK model, did not result in a proportional 2-fold increase in PI's maternal clearance. Instead, the increase was rather modest, 1.1-fold for DRV and 1.5-fold for LPV. The reason for this observation is likely due to inhibition of hepatic (and intestinal) CYP3A enzymes by RTV (Kirby et al., 2011). And, incorporation of such inhibition in our m-f PBPK recapitulated the observed increase in maternal clearance of 1.2-fold and 1.4-fold, respectively (**Figure 2 B-D, 3 B-D**)**.** Finally, our prediction of $K_{p,uu}$ was based on UV/MP values, values that are obtained from

DMD Fast Forward. Published on August 23, 2021 as DOI: 10.1124/dmd.121.000538
This article has not been copyedited and formatted. The final version may differ from this version.

multiple maternal-fetal dyads, rather than on UV values alone. This is because significant inter-individual variability in maternal plasma concentration can result in significant inter-individual variability in UV C-T profile. However, this variability is considerably mitigated when UV/MP values are used.

Our *in vitro* findings confirmed previous data (Crowe & Tan, 2012; Prasad & Unadkat, 2015; Ueda et al., 1992) that all four drugs are moderate to excellent P-gp substrates (defined by FDA as efflux ratios of >2 in P-gp overexpressing cell lines(Administration, 2017)) (**Figure 2, Table 1**). As expected, because DEX and BET are epimers, their efflux ratios in the P-gp overexpressing cell line and the corresponding predicted fetal $K_{p,uu}$ were not significantly different (**Figure 2A, Table 1**), consistent with their similar *in vivo* $K_{p,uu}$ (manuscript in press). Based on these data, the estimated *in vivo* $f_{t,P\text{-}gp}$ for DEX and BET were 0.52 and 0.50, respectively. LPV showed higher ER (hence, lower ER-REF predicted $K_{p,uu}$, or alternatively, higher $f_{t,P\text{-}gp}$) than DRV (**Figure 2B, Table 1**). Hence, our *in vitro* predictions (in agreement with DRV and LPV *in vivo* $K_{p,uu}$ observations – **Figure 3 E-F, 4 E-F,** respectively) indicate lower fetal LPV exposure at term compared to DRV. Also, placental P-gp drug efflux resulted in decreased fetal drug exposure to all four drugs ($K_{p,uu} < 1$, **Figure 5**) when compared with their corresponding fetal exposure ($K_{p,uu} = 1$) if only passive placental diffusion of the drug was assumed.

The mean ER-REF predicted $K_{p,uu}$ values were in good to excellent agreement with the estimated *in vivo* $K_{p,uu}$ values demonstrating success of the ER-REF approach (**Figure 5, Table 1**). For DEX and BET, the observed *in vivo* $K_{p,uu}$ was modestly overpredicted by the ER-REF approach. This success enhances confidence in using our ER-REF approach to predict fetal exposure to drugs at earlier gestational ages. This is important because many drugs (e.g., DRV,

DMD Fast Forward. Published on August 23, 2021 as DOI: 10.1124/dmd.121.000538
This article has not been copyedited and formatted. The final version may differ from this version.

LPV) are administered to pregnant women earlier in gestation and/or throughout pregnancy. Indeed, our m-f PBPK model predicted lower fetal exposure to DRV or LPV at GW20 vs. term (**Figure 6**). This finding is a result of an interplay between two clearance processes defining transplacental passage of the drugs (**Eq. 4**). Alternatively stated, it is the ratio of $CL_{int,P\text{-}gp,placenta}$ and $CL_{int,PD,placenta}$ that determines $K_{p,uu}$ of drugs. Although P-gp abundance per gram of placenta is higher at GW20 vs. term, because the placenta size is smaller at GW20 vs. term, the abundance of P-gp in the whole placenta is also lower at GW20 vs. term. Both the size and total placental P-gp abundance at GW20 vs. term resulted in a greater decrease in $CL_{int,PD,placenta}$ of the drugs (↓80%, due to lower placental surface area) than in the decrease in $CL_{int,P\text{-}gp,placenta}$ (↓40%, due to lower total P-gp abundance) resulting in lower predicted *in vivo* $K_{p,uu}$ of the drugs at GW20 vs. term. Unfortunately, the predicted fetal drug exposure at GW20 cannot be verified due to the lack of observed UV data. Nevertheless, these predictions demonstrate the ability of our m-f PBPK model to predict fetal exposure to drugs at earlier gestational ages.

There are several limitations to our study. First, verification of LPV $K_{p,uu}$ was challenging because of the large variability in the maternal-fetal data. Hence, we resorted to the use of previously published PopPK model predictions. When data for additional drugs appropriate for PBPK modeling are available (criteria for such data sets were described before in the manuscript **in press**), we will be able to verify our model with greater confidence and for additional P-gp substrates. Second, we modestly overpredicted DEX UV/MP ratio profile based on the ER-REF predicted $K_{p,uu}$ value (**Figure S4D**). This over-prediction may be due to lack of observed UV/MP values over a duration necessary to accurately estimate its $K_{p,uu,}$ involvement of efflux transporters other than P-gp or BCRP or metabolism in the placenta. Third, we could not

predict fetal exposure to drugs at <GW20 as fetal physiological parameters are not reliably available at <GW20 (Abduljalil, Jamei, & Johnson, 2018; Zhang et al., 2017). Additionally, the lack of established maternal-placental blood circulation before GW13 (Chang, Wakeland, & Parast, 2018) (restricting overall drug access to the fetus), limits out model application to the second and third trimester of pregnancy.

Despite the high prevalence of drug use in pregnancy (~80% of pregnant women using at least one drug (Scaffidi et al., 2017)), 90% of drugs on the market still lack guidance on their administration in this population, leaving both mother and her fetus “drug orphans”. Although we have some understanding of maternal drug exposure (and changes therein) during pregnancy (Abduljalil, Furness, Johnson, Rostami-Hodjegan, & Soltani, 2012; Abduljalil, Pansari, & Jamei, 2020; Anderson, 2005; Hebert et al., 2008), this is not the case for fetal drug exposure which is related to fetal drug efficacy and toxicity. This study is the first to address this significant gap in health care knowledge, that is development of a method to successfully predict fetal exposure to drugs irrespective of whether they are transported or not. Since, UV/MP data at term are not readily available for all drugs prescribed to pregnant women, and since such studies are logistically and ethically challenging to conduct, our approach provides a means to predict fetal exposure to drugs, irrespective of whether they diffuse across the placenta or are transported. Moreover, together with placental transporter abundance that we have previously quantified (Anoshchenko et al., 2020), this ER-REF approach can be used to predict fetal exposure to placental transported drugs at gestational ages other than term (as shown here for GW20). Our ER-REF scaling approach can easily be adapted to substrates of multiple placental transporters (e.g., P-gp and/or BCRP) as has been shown before for

transporter-mediated uptake and distribution of drugs to various organs (Ishida et al., 2018; A. R. Kumar et al., 2021; V. Kumar et al., 2018; Sachar et al., 2020; Storelli et al., 2021; Trapa, Belova, Liras, Scott, & Steyn, 2016; Trapa et al., 2019). In conclusion, our study provides a tool to prospectively predict the fetal exposure to drugs at various gestational ages to help assess potential fetal benefits and risks associated with maternal drug administration.

DMD Fast Forward. Published on August 23, 2021 as DOI: 10.1124/dmd.121.000538
This article has not been copyedited and formatted. The final version may differ from this version.

ACKNOWLEDGEMENTS

We would like to thank Dr. Artursson (University of Uppsala, Sweden) and Dr. Mao (University of Washington) for generously providing hMDR1-MDCK$^{cP\text{-}gpKO}$ and hABCG2-MDCKII cells, respectively; Dr. Maharao and Dr. Sachar for help with establishing the Transwell® assay, Dale Wittington and Scott Edgar for help with mass spectrometry analysis, and the University of Washington Pharmacokinetics of Drug Abuse during Pregnancy (UWPKDAP) program for informative discussions.

DMD Fast Forward. Published on August 23, 2021 as DOI: 10.1124/dmd.121.000538
This article has not been copyedited and formatted. The final version may differ from this version.

AUTHORSHIP CONTRIBUTIONS

Participated in research design: Anoshchenko, Storelli, Unadkat

Conducted experiments: Anoshchenko

Performed data analysis: Anoshchenko, Storelli

Wrote or contributed to the writing of the manuscript: Anoshchenko, Storelli, Unadkat

REFERENCES

Abduljalil, K., Furness, P., Johnson, T. N., Rostami-Hodjegan, A., & Soltani, H. (2012). Anatomical, physiological and metabolic changes with gestational age during normal pregnancy: a database for parameters required in physiologically based pharmacokinetic modelling. *Clin Pharmacokinet, 51*(6), 365-396. doi:10.2165/11597440-000000000-00000

Abduljalil, K., Jamei, M., & Johnson, T. N. (2018). Fetal Physiologically Based Pharmacokinetic Models: Systems Information on the Growth and Composition of Fetal Organs. *Clin Pharmacokinet*. doi:10.1007/s40262-018-0685-y

Abduljalil, K., Pansari, A., & Jamei, M. (2020). Prediction of maternal pharmacokinetics using physiologically based pharmacokinetic models: assessing the impact of the longitudinal changes in the activity of CYP1A2, CYP2D6 and CYP3A4 enzymes during pregnancy. *J Pharmacokinet Pharmacodyn, 47*(4), 361-383. doi:10.1007/s10928-020-09711-2

Administration, U. F. a. D. (2017). *In Vitro Metabolism and Transporter Mediated Drug-Drug Interaction Studies: Guidance for Industry (FDA)*. Silver Spring, MD.

Agarwal, S., Pal, D., & Mitra, A. K. (2007). Both P-gp and MRP2 mediate transport of Lopinavir, a protease inhibitor. *Int J Pharm, 339*(1-2), 139-147. doi:10.1016/j.ijpharm.2007.02.036

Anderson, G. D. (2005). Pregnancy-induced changes in pharmacokinetics: a mechanistic-based approach. *Clin Pharmacokinet, 44*(10), 989-1008. doi:10.2165/00003088-200544100-00001

Anoshchenko, O., Prasad, B., Neradugomma, N. K., Wang, J., Mao, Q., & Unadkat, J. D. (2020). Gestational Age-Dependent Abundance of Human Placental Transporters as Determined by Quantitative Targeted Proteomics. *Drug Metab Dispos, 48*(9), 735-741. doi:10.1124/dmd.120.000067

Arumugasaamy, N., Rock, K. D., Kuo, C. Y., Bale, T. L., & Fisher, J. P. (2020). Microphysiological systems of the placental barrier. *Adv Drug Deliv Rev*. doi:10.1016/j.addr.2020.08.010

Billington, S., Salphati, L., Hop, C., Chu, X., Evers, R., Burdette, D., . . . Unadkat, J. D. (2019). Interindividual and Regional Variability in Drug Transporter Abundance at the Human Blood-Brain Barrier Measured by Quantitative Targeted Proteomics. *Clin Pharmacol Ther, 106*(1), 228-237. doi:10.1002/cpt.1373

Blanford, A. T., & Murphy, B. E. (1977). In vitro metabolism of prednisolone, dexamethasone, betamethasone, and cortisol by the human placenta. *Am J Obstet Gynecol, 127*(3), 264-267.

Boffito, M., Miralles, D., & Hill, A. (2008). Pharmacokinetics, efficacy, and safety of darunavir/ritonavir 800/100 mg once-daily in treatment-naive and -experienced patients. *HIV Clin Trials, 9*(6), 418-427. doi:10.1310/hct0906-418

Chang, C. W., Wakeland, A. K., & Parast, M. M. (2018). Trophoblast lineage specification, differentiation and their regulation by oxygen tension. *J Endocrinol, 236*(1), R43-R56. doi:10.1530/JOE-17-0402

Colbers, A., Greupink, R., Litjens, C., Burger, D., & Russel, F. G. (2016). Physiologically Based Modelling of Darunavir/Ritonavir Pharmacokinetics During Pregnancy. *Clin Pharmacokinet, 55*(3), 381-396. doi:10.1007/s40262-015-0325-8

Colbers, A., Molto, J., Ivanovic, J., Kabeya, K., Hawkins, D., Gingelmaier, A., . . . Network, P. (2015). Pharmacokinetics of total and unbound darunavir in HIV-1-infected pregnant women. *J Antimicrob Chemother, 70*(2), 534-542. doi:10.1093/jac/dku400

Cressey, T. R., Urien, S., Capparelli, E. V., Best, B. M., Buranabanjasatean, S., Limtrakul, A., . . . Mirochnick, M. (2015). Impact of body weight and missed doses on lopinavir concentrations with standard and increased lopinavir/ritonavir doses during late pregnancy. *J Antimicrob Chemother, 70*(1), 217-224. doi:10.1093/jac/dku367

Crowe, A., & Tan, A. M. (2012). Oral and inhaled corticosteroids: differences in P-glycoprotein (ABCB1) mediated efflux. *Toxicol Appl Pharmacol, 260*(3), 294-302. doi:10.1016/j.taap.2012.03.008

Eron, J. J., Feinberg, J., Kessler, H. A., Horowitz, H. W., Witt, M. D., Carpio, F. F., . . . Sun, E. (2004). Once-daily versus twice-daily lopinavir/ritonavir in antiretroviral-naive HIV-positive patients: a 48-week randomized clinical trial. *J Infect Dis, 189*(2), 265-272. doi:10.1086/380799

Fauchet, F., Treluyer, J. M., Illamola, S. M., Pressiat, C., Lui, G., Valade, E., . . . Hirt, D. (2015). Population approach to analyze the pharmacokinetics of free and total lopinavir in HIV-infected pregnant women and consequences for dose adjustment. *Antimicrob Agents Chemother, 59*(9), 5727-5735. doi:10.1128/AAC.00863-15

Gimenez, F., Fernandez, C., & Mabondzo, A. (2004). Transport of HIV protease inhibitors through the blood-brain barrier and interactions with the efflux proteins, P-glycoprotein and multidrug resistance proteins. *J Acquir Immune Defic Syndr, 36*(2), 649-658. doi:10.1097/00126334-200406010-00001

Hebert, M. F., Easterling, T. R., Kirby, B., Carr, D. B., Buchanan, M. L., Rutherford, T., . . . Unadkat, J. D. (2008). Effects of pregnancy on CYP3A and P-glycoprotein activities as measured by disposition of midazolam and digoxin: a University of Washington specialized center of research study. *Clin Pharmacol Ther, 84*(2), 248-253. doi:10.1038/clpt.2008.1

Huisman, M. T., Smit, J. W., Wiltshire, H. R., Hoetelmans, R. M., Beijnen, J. H., & Schinkel, A. H. (2001). P-glycoprotein limits oral availability, brain, and fetal penetration of saquinavir even with high doses of ritonavir. *Mol Pharmacol, 59*(4), 806-813.

Ishida, K., Ullah, M., Toth, B., Juhasz, V., & Unadkat, J. D. (2018). Successful Prediction of In Vivo Hepatobiliary Clearances and Hepatic Concentrations of Rosuvastatin Using Sandwich-Cultured Rat Hepatocytes, Transporter-Expressing Cell Lines, and Quantitative Proteomics. *Drug Metab Dispos, 46*(1), 66-74. doi:10.1124/dmd.117.076539

Joshi, A. A., Vaidya, S. S., St-Pierre, M. V., Mikheev, A. M., Desino, K. E., Nyandege, A. N., . . . Gerk, P. M. (2016). Placental ABC Transporters: Biological Impact and Pharmaceutical Significance. *Pharm Res, 33*(12), 2847-2878. doi:10.1007/s11095-016-2028-8

Ke, A. B., Nallani, S. C., Zhao, P., Rostami-Hodjegan, A., & Unadkat, J. D. (2012). A PBPK Model to Predict Disposition of CYP3A-Metabolized Drugs in Pregnant Women: Verification and Discerning the Site of CYP3A Induction. *CPT Pharmacometrics Syst Pharmacol, 1*, e3. doi:10.1038/psp.2012.2

Ke, A. B., Nallani, S. C., Zhao, P., Rostami-Hodjegan, A., & Unadkat, J. D. (2014). Expansion of a PBPK model to predict disposition in pregnant women of drugs cleared via multiple CYP enzymes, including CYP2B6, CYP2C9 and CYP2C19. *Br J Clin Pharmacol, 77*(3), 554-570. doi:10.1111/bcp.12207

Kirby, B. J., Collier, A. C., Kharasch, E. D., Whittington, D., Thummel, K. E., & Unadkat, J. D. (2011). Complex drug interactions of HIV protease inhibitors 1: inactivation, induction, and inhibition of cytochrome P450 3A by ritonavir or nelfinavir. *Drug Metab Dispos, 39*(6), 1070-1078. doi:10.1124/dmd.110.037523

Konig, S. K., Herzog, M., Theile, D., Zembruski, N., Haefeli, W. E., & Weiss, J. (2010). Impact of drug transporters on cellular resistance towards saquinavir and darunavir. *J Antimicrob Chemother, 65*(11), 2319-2328. doi:10.1093/jac/dkq324

Kumar, A. R., Prasad, B., Bhatt, D. K., Mathialagan, S., Varma, M. V. S., & Unadkat, J. D. (2021). IVIVE of Transporter-Mediated Renal Clearance: Relative Expression Factor (REF) vs Relative Activity Factor (RAF) Approach. *Drug Metab Dispos*. doi:10.1124/dmd.121.000367

Kumar, V., Yin, J., Billington, S., Prasad, B., Brown, C. D. A., Wang, J., & Unadkat, J. D. (2018). The Importance of Incorporating OCT2 Plasma Membrane Expression and Membrane Potential in IVIVE of Metformin Renal Secretory Clearance. *Drug Metab Dispos, 46*(10), 1441-1445. doi:10.1124/dmd.118.082313

Mathias, A. A., Hitti, J., & Unadkat, J. D. (2005). P-glycoprotein and breast cancer resistance protein expression in human placentae of various gestational ages. *Am J Physiol Regul Integr Comp Physiol, 289*(4), R963-969. doi:10.1152/ajpregu.00173.2005

Murphy, V. E., Fittock, R. J., Zarzycki, P. K., Delahunty, M. M., Smith, R., & Clifton, V. L. (2007). Metabolism of synthetic steroids by the human placenta. *Placenta, 28*(1), 39-46. doi:10.1016/j.placenta.2005.12.010

Murtagh, R., Else, L. J., Kuan, K. B., Khoo, S. H., Jackson, V., Patel, A., . . . Lambert, J. S. (2019). Therapeutic drug monitoring of darunavir/ritonavir in pregnancy. *Antivir Ther*. doi:10.3851/IMP3291

Myllynen, P., Immonen, E., Kummu, M., & Vahakangas, K. (2009). Developmental expression of drug metabolizing enzymes and transporter proteins in human placenta and fetal tissues. *Expert Opin Drug Metab Toxicol, 5*(12), 1483-1499. doi:10.1517/17425250903304049

Myllynen, P., Pasanen, M., & Vahakangas, K. (2007). The fate and effects of xenobiotics in human placenta. *Expert Opin Drug Metab Toxicol, 3*(3), 331-346. doi:10.1517/17425255.3.3.331

Pasanen, M. (1999). The expression and regulation of drug metabolism in human placenta. *Adv Drug Deliv Rev, 38*(1), 81-97. doi:10.1016/s0169-409x(99)00008-3

Petersen, M. C., Nation, R. L., Ashley, J. J., & McBride, W. G. (1980). The placental transfer of betamethasone. *Eur J Clin Pharmacol, 18*(3), 245-247.

Prasad, B., & Unadkat, J. D. (2015). The concept of fraction of drug transported (ft) with special emphasis on BBB efflux of CNS and antiretroviral drugs. *Clin Pharmacol Ther, 97*(4), 320-323. doi:10.1002/cpt.72

Russell, M. A., Carpenter, M. W., Akhtar, M. S., Lagattuta, T. F., & Egorin, M. J. (2007). Imatinib mesylate and metabolite concentrations in maternal blood, umbilical cord blood, placenta and breast milk. *J Perinatol, 27*(4), 241-243. doi:10.1038/sj.jp.7211665

Sachar, M., Kumar, V., Gormsen, L. C., Munk, O. L., & Unadkat, J. D. (2020). Successful Prediction of Positron Emission Tomography-Imaged Metformin Hepatic Uptake Clearance in Humans Using the Quantitative Proteomics-Informed Relative Expression Factor Approach. *Drug Metab Dispos, 48*(11), 1210-1216. doi:10.1124/dmd.120.000156

Scaffidi, J., Mol, B. W., & Keelan, J. A. (2017). The pregnant women as a drug orphan: a global survey of registered clinical trials of pharmacological interventions in pregnancy. *BJOG, 124*(1), 132-140. doi:10.1111/1471-0528.14151

Schinkel, A. H., & Jonker, J. W. (2003). Mammalian drug efflux transporters of the ATP binding cassette (ABC) family: an overview. *Adv Drug Deliv Rev, 55*(1), 3-29. doi:10.1016/s0169-409x(02)00169-2

Sekar, V., Spinosa-Guzman, S., De Paepe, E., Stevens, T., Tomaka, F., De Pauw, M., & Hoetelmans, R. M. (2010). Pharmacokinetics of multiple-dose darunavir in combination with low-dose ritonavir in individuals with mild-to-moderate hepatic impairment. *Clin Pharmacokinet, 49*(5), 343-350. doi:10.2165/11530690-000000000-00000

Sekar, V. J., Lefebvre, E., De Pauw, M., Vangeneugden, T., & Hoetelmans, R. M. (2008). Pharmacokinetics of darunavir/ritonavir and ketoconazole following co-administration in HIV-healthy volunteers. *Br J Clin Pharmacol, 66*(2), 215-221. doi:10.1111/j.1365-2125.2008.03191.x

Sheffield, J. S., Siegel, D., Mirochnick, M., Heine, R. P., Nguyen, C., Bergman, K. L., . . . Nesin, M. (2014). Designing drug trials: considerations for pregnant women. *Clin Infect Dis, 59 Suppl 7*, S437-444. doi:10.1093/cid/ciu709

Stek, A., Best, B. M., Wang, J., Capparelli, E. V., Burchett, S. K., Kreitchmann, R., . . . Mirochnick, M. (2015). Pharmacokinetics of Once Versus Twice Daily Darunavir in Pregnant HIV-Infected Women. *J Acquir Immune Defic Syndr, 70*(1), 33-41. doi:10.1097/QAI.0000000000000668

Storelli, F., Anoshchenko, O., & Unadkat, J. D. (2021). Successful prediction of human brain Kp,uu of P-gp substrates using the proteomics-informed relative expression factor approach. *Clin Pharmacol Ther*. doi:10.1002/cpt.2227

Storelli, F., Billington, S., Kumar, A. R., & Unadkat, J. D. (2020). Abundance of P-Glycoprotein and Other Drug Transporters at the Human Blood-Brain Barrier in Alzheimer's Disease: A Quantitative Targeted Proteomic Study. *Clin Pharmacol Ther*. doi:10.1002/cpt.2035

Tayrouz, Y., Ganssmann, B., Ding, R., Klingmann, A., Aderjan, R., Burhenne, J., . . . Mikus, G. (2001). Ritonavir increases loperamide plasma concentrations without evidence for P-glycoprotein involvement. *Clin Pharmacol Ther, 70*(5), 405-414. doi:10.1067/mcp.2001.119212

Trapa, P. E., Belova, E., Liras, J. L., Scott, D. O., & Steyn, S. J. (2016). Insights From an Integrated Physiologically Based Pharmacokinetic Model for Brain Penetration. *J Pharm Sci, 105*(2), 965-971. doi:10.1016/j.xphs.2015.12.005

Trapa, P. E., Troutman, M. D., Lau, T. Y., Wager, T. T., Maurer, T. S., Patel, N. C., . . . Liras, J. L. (2019). In vitro-In vivo extrapolation of key transporter activity at the blood-brain barrier. *Drug Metab Dispos*. doi:10.1124/dmd.118.083279

Tsuei, S. E., Petersen, M. C., Ashley, J. J., McBride, W. G., & Moore, R. G. (1980). Disporition of synthetic glucocorticoids. II. Dexamethasone in parturient women. *Clin Pharmacol Ther, 28*(1), 88-98.

Uchida, Y., Ohtsuki, S., Kamiie, J., & Terasaki, T. (2011). Blood-brain barrier (BBB) pharmacoproteomics: reconstruction of in vivo brain distribution of 11 P-glycoprotein substrates based on the BBB transporter protein concentration, in vitro intrinsic transport activity, and unbound fraction in plasma and brain in mice. *J Pharmacol Exp Ther, 339*(2), 579-588. doi:10.1124/jpet.111.184200

Uchida, Y., Wakayama, K., Ohtsuki, S., Chiba, M., Ohe, T., Ishii, Y., & Terasaki, T. (2014). Blood-brain barrier pharmacoproteomics-based reconstruction of the in vivo brain distribution of P-glycoprotein substrates in cynomolgus monkeys. *J Pharmacol Exp Ther, 350*(3), 578-588. doi:10.1124/jpet.114.214536

Ueda, K., Okamura, N., Hirai, M., Tanigawara, Y., Saeki, T., Kioka, N., . . . Hori, R. (1992). Human P-glycoprotein transports cortisol, aldosterone, and dexamethasone, but not progesterone. *J Biol Chem, 267*(34), 24248-24252.

Vermeer, L. M., Isringhausen, C. D., Ogilvie, B. W., & Buckley, D. B. (2016). Evaluation of Ketoconazole and Its Alternative Clinical CYP3A4/5 Inhibitors as Inhibitors of Drug Transporters: The In Vitro Effects of Ketoconazole, Ritonavir, Clarithromycin, and Itraconazole on 13 Clinically-Relevant Drug Transporters. *Drug Metab Dispos, 44*(3), 453-459. doi:10.1124/dmd.115.067744

Wagner, C., Zhao, P., Arya, V., Mullick, C., Struble, K., & Au, S. (2017). Physiologically Based Pharmacokinetic Modeling for Predicting the Effect of Intrinsic and Extrinsic Factors on Darunavir or Lopinavir Exposure Coadministered With Ritonavir. *J Clin Pharmacol, 57*(10), 1295-1304. doi:10.1002/jcph.936

Zhang, Z., Farooq, M., Prasad, B., Grepper, S., & Unadkat, J. D. (2015). Prediction of gestational age-dependent induction of in vivo hepatic CYP3A activity based on HepaRG cells and human hepatocytes. *Drug Metab Dispos, 43*(6), 836-842. doi:10.1124/dmd.114.062984

Zhang, Z., Imperial, M. Z., Patilea-Vrana, G. I., Wedagedera, J., Gaohua, L., & Unadkat, J. D. (2017). Development of a Novel Maternal-Fetal Physiologically Based Pharmacokinetic Model I: Insights into Factors that Determine Fetal Drug Exposure through Simulations and Sensitivity Analyses. *Drug Metab Dispos, 45*(8), 920-938. doi:10.1124/dmd.117.075192

Zhang, Z., & Unadkat, J. D. (2017). Development of a Novel Maternal-Fetal Physiologically Based Pharmacokinetic Model II: Verification of the model for passive placental permeability drugs. *Drug Metab Dispos, 45*(8), 939-946. doi:10.1124/dmd.116.073957

FOOTNOTES

This work was supported by a Bill & Melinda Gates Foundation Grant [INV-006678] and a NIH grant [P01 DA032507].

All authors declare no conflict of interest.

DMD Fast Forward. Published on August 23, 2021 as DOI: 10.1124/dmd.121.000538
This article has not been copyedited and formatted. The final version may differ from this version.

LEGENDS FOR FIGURES

Figure 1. Workflow for the prediction *in vivo* fetal $K_{p,uu}$ using the ER-REF approach and subsequent verification of the predicted $K_{p,uu}$ by comparison with the observed *in vivo* $K_{p,uu}$ estimated by m-f PBPK modeling and simulation. Top panel: Efflux transporter-overexpressing cell monolayer (e.g., hMDR1-MDCK$^{cP\text{-}gp\ KO}$) in the *in vitro* Transwell® system (1) mimics the placental syncytiotrophoblast (SYT) layer *in vivo* (2). That is, the apical and basal chambers in the *in vitro* system, respectively, mimic the *in vivo* maternal and fetal blood compartments allowing the use of the ER-REF approach to predict the *in vivo* fetal $K_{p,uu}$. For verification, this predicted $K_{p,uu}$ was compared with the observed *in vivo* $K_{p,uu}$ estimated by m-f PBPK modeling and simulation as depicted in the bottom panel. Orange arrows indicate bidirectional intrinsic passive diffusion clearance. Blue circles and blue arrows respectively represent apically localized efflux transporters and the direction of drug efflux/ intrinsic placental-maternal clearance (CL_{PM}, specified as $CL_{int,P\text{-}gp,placenta}$ in the text). ER-REF is efflux ratio-relative expression factor approach. $P_{app(B\rightarrow A)}$ and $P_{app(A\rightarrow B)}$ are apparent permeabilities and $CL_{int(B\rightarrow A)}$ and $CL_{int(A\rightarrow B)}$ are apparent intrinsic clearances of a drug in the indicated directions. **Bottom panel**: Estimation of $K_{p,uu}$ from the observed *in vivo* data with and without intrinsic active placental-maternal efflux clearance (CL_{PM}) incorporated into the model. For drugs that are effluxed by placental P-gp (i.e., $CL_{PM}>0$), CL_{PM} was adjusted until the m-f PBPK model-predicted UV/MP values best described the observed UV/MP values (dots). Then, based on **Eq 1** the *in vivo* $K_{p,uu}$ was estimated. CL_{PD}: intrinsic passive diffusion clearance; CL_{FP}, CL_{PF}, CL_{MP}: intrinsic active fetal-placental, placental-fetal and maternal-placental clearances, respectively (assume 0 for drugs

DMD Fast Forward. Published on August 23, 2021 as DOI: 10.1124/dmd.121.000538
This article has not been copyedited and formatted. The final version may differ from this version.

transported only by placental-maternal efflux transporters (CL_{PM})); ROM: rest of the maternal compartments, ROF: rest of the fetal compartments, UV: umbilical vein; UA: umbilical artery.

Figure 2. Efflux ratios (ER) of test compounds in Transwell assays using monolayer of (A, B) hMDR1-MDCK$^{cP\text{-}gp\ KO}$ or (C) hABCG2-MDCKII. All four drugs were substrates of P-gp in hMDR1-MDCK$^{cP\text{-}gp\ KO}$ cells as evidenced by their P-gp mediated efflux ratio, $ER_{P\text{-}gp}$ (i.e., $ER_{P\text{-}gp} = ER_{TRQ(-)} - ER_{TRQ(+)}$ where TRQ is tariquidar). **(A)** $ER_{P\text{-}gp}$ of DEX (5.1±1.2) and BET (6.1±1.3) were not significantly different, (Kruskal-Wallis test). **(B)** while the $ER_{P\text{-}gp}$ of LPV (83.1±10.1) and DRV (39.3±1.8) were significantly different from each other and greater than those of DEX and BET **(C)** neither DEX nor BET were substrates of BCRP in hABCG2-MDCKII cells (in the absence of KO143) as evidenced by their efflux ratios of 1.2±0.3 and 1.1±0.1, respectively. Drug concentrations in the donor compartments were 2 µM for DEX, BET and DRV, and 1 µM for LPV. Dots represent individual experiments, each conducted in triplicate; lines represent means and standard deviations. Detailed summary of the efflux ratios of test compounds is provided in **Table 1.**

Figure 3. PBPK predictions of DRV steady-state plasma concentrations in (A1) non-pregnant individuals, (B1) pregnant women at GW 34 (intensively sampled), (C1) pregnant women at GW 38 (sparsely sampled) and their (D1) fetuses at GW38 (sparsely sampled) and (E1) umbilical venous (UV)/maternal plasma (MP) ratio at GW38 with and without incorporation of placental P-gp efflux. Subjects were administered DRV/RTV 600/100 mg PO BID. (A1)

DMD Fast Forward. Published on August 23, 2021 as DOI: 10.1124/dmd.121.000538
This article has not been copyedited and formatted. The final version may differ from this version.

SimCYP® or **(B1, C1)** m-f PBPK predicted mean concentration-time profile (solid line) and $CI_{90\%}$ (dashed lines) are overlaid on the observed data (intensively sampled, **A1**, circles: mean ± SD, n=8; **B1**, circles: mean ± SD, n=32, triangles: mean ± SD, n=6; or **(C1)** sparsely-sampled). **(D1, D2)** The observed fetal UV concentration-time data were better predicted by our m-f PBPK model in the presence of P-gp efflux clearance ($K_{p,uu}$ =0.16 - black solid line; dashed lines - 5th and 95th percentile profiles) vs. in the absence of P-gp efflux clearance (i.e., passive diffusion only resulting in $K_{p,uu}$=1 - grey solid line). **(E1)** The m-f PBPK model better predicted UV/MP ratios in the presence of P-gp efflux clearance ($K_{p,uu}$= 0.16) vs. in the absence of P-gp efflux clearance ($K_{p,uu}$= 1). The observed UV/MP ratios are combined from two dosing regimens of DRV/RTV: 600/100 BID and 800/100 QD to increase the confidence in our model verification as these ratios are independent of dosing regimen. **(A2, B2, D2, E2)** The predicted pharmacokinetic parameters in **A2, B2** met our *a priori* defined acceptance criteria (within 0.8-1.25 fold of the observed data). The observed PK parameters were estimated from Stek *et al*., 2015 (*) or Colbers *et al*., 2015 (†).

Figure 4. PBPK predictions of LPV steady-state plasma concentrations in (A1) non-pregnant individuals, (B1) pregnant women and (C1) their fetuses at GW38 and (D1) umbilical venous (UV)/maternal plasma (MP) ratio with and without incorporation of placental P-gp efflux. Subjects were administered LPV/RTV 400/100 mg PO BID. (A1, B1) SimCYP® or m-f PBPK predicted mean concentration-time profile (solid line) and $CI_{90\%}$ (dashed lines) are overlaid on the observed data (**A1** - circles: mean ± SD, n=19; squares: mean ± SD, n=16) or **B1**, two published population pharmacokinetic (PopPK) profiles respectively (grey solid line). **(C1, C2)**

DMD Fast Forward. Published on August 23, 2021 as DOI: 10.1124/dmd.121.000538
This article has not been copyedited and formatted. The final version may differ from this version.

The "observed" (i.e., PopPK predicted) fetal UV concentration-time profile (dotted line) was better predicted by our m-f PBPK model in the presence of P-gp efflux clearance ($K_{p,uu}$ =0.11 - black solid line; dashed lines - 5th and 95th percentile profiles) vs. in the absence of P-gp efflux clearance (i.e., passive diffusion only resulting in $K_{p,uu}$=1 - grey solid line). **(D1)** The m-f PBPK model better predicted the "observed" (i.e., PopPK predicted) UV/MP ratios in the presence of P-gp efflux clearance ($K_{p,uu}$= 0.11) vs. in the absence of P-gp efflux clearance ($K_{p,uu}$= 1). **(A2, B2, C2, D2)** The predicted pharmacokinetic parameters met our *a priori* defined acceptance criteria (within 0.8-1.25 of the observed or PopPK predicted). The published PopPK parameters were estimated from **(A2)** Eron *et al*., 2004 (*) and Scholler-Gyure et al., 2013 (†), or **(B2)** Fauchet et al., 2015 (*) or Cressey et al., 2015 (†).

Figure 5. Successful prediction of fetal $K_{p,uu}$ by the REF-ER approach when compared with the *in vivo* $K_{p,uu}$ estimated by m-f PBPK modeling and simulation of the observed data. The mean ER-REF predicted $K_{p,uu}$ values of DEX, BET, DRV and LPV (green bars, error bars are $CI_{90\%}$) fell within $CI_{90\%}$ (error bars) of the mean observed values (grey bar), demonstrating the success of the ER-REF approach.

Figure 6. M-f PBPK model predictions of DRV or LPV steady-state plasma drug concentrations at gestational week 20 (GW20) after administration of (A-C) 600/100 mg PO DRV/RTV BID or (D-F) 400/100 mg PO LPV/RTV BID. (B, C) Fetal plasma DRV C_{max} and AUC_{0-12} at GW20 were 45% and 43% of that at GW38 (**Figure 3 D1, D2**), while maternal plasma DRV C_{max} and AUC_{0-12} at

DMD Fast Forward. Published on August 23, 2021 as DOI: 10.1124/dmd.121.000538
This article has not been copyedited and formatted. The final version may differ from this version.

GW20 **(A, C)** were approximately the same as that at GW38 (**Figure 3 B1, B2**), indicating that both P-gp efflux and passive diffusion clearance affect fetal rather than maternal DRV exposure. These values yielded DRV $K_{p,uu}$ of 0.11 at GW20 vs. $K_{p,uu}$ of 0.16 at GW38. **(B-inset, C)** DRV UV/MP ratio at GW20 was 41% of that at GW38 (**Figure 3 E1, E2**). **(E, F)** Fetal plasma LPV C_{max} and $AUC_{0\text{-}12}$ at GW20 were 41% and 38% of that at GW38 (**Figure 4 C1, C2**), while maternal plasma LPV C_{max} and $AUC_{0\text{-}12}$ at GW20 **(D, F)** were only modestly (1.12 and 1.15-fold, respectively) higher than at GW38 (**Figure 4 B1, B2**). These valued yielded LPV $K_{p,uu}$=0.07 at GW20 vs. $K_{p,uu}$ of 0.11 at GW38. **(E-inset, F)** LPV UV/MP ratio at GW20 was 29% of that at GW38 (**Figure 4 D1, D2**).

TABLES

Table 1. ER, REF and the predicted fetal $K_{p,uu}$ for P-gp Substrates using the ER-REF approach and P-gp overexpressing cells (hMDR1-MDCK$^{cP\text{-}gp\ KO}$).

Drug	Exp #	$ER_{TRQ(-)}$	$ER_{TRQ(+)}$	$ER_{P\text{-}gp}$	*In vitro* P-gp abundance (pmol/mg HP)	REF	Predicted $K_{p,uu}$		Observed $K_{p,uu}$	Predicted / Observed
				$ER_{TRQ(-)}$ - $ER_{TRQ(+)}$			Value	Mean ($CI_{90\%}$)	Mean ($CI_{90\%}$)	
DEX	1	5.42	0.85	4.58	1.16	0.14	0.61	0.63 (0.48 - 0.78)	0.48 (0.30 - 0.66)	1.31
	2	5.37	1.04	4.33	1.34	0.12	0.66			
	3	8.33	1.35	6.99	1.92	0.08	0.63			
	4	5.65	0.90	4.75	1.20	0.13	0.61			
	Mean ± SD	6.2 ± 1.43	1.03 ± 0.22	5.16 ± 1.23	1.41 ± 0.35	0.12 ± 0.02				
BET	1	6.56	0.95	5.61	1.16	0.14	0.56	0.59 (0.42 - 0.69)	0.5 (0.29 - 0.71)	1.18
	2	5.64	1.07	4.57	1.34	0.12	0.65			
	3	8.64	1.03	7.62	1.92	0.08	0.62			
	4	7.66	0.92	6.74	1.20	0.13	0.53			
	Mean ± SD	7.13 ± 1.31	0.99 ± 0.07	6.13 ± 1.33	1.41 ± 0.35	0.12 ± 0.03				
DRV	1	40.43	0.82	39.61	1.16	0.14	0.15	0.17 (0.10 - 0.23)	0.16 (0.11 - 0.22)	1.06
	2	41.83	1.48	40.35	1.34	0.12	0.17			

	3	37.86	1.12	36.74	1.92	0.08	0.25			
	4	41.73	1.06	40.67	1.20	0.13	0.16			
	Mean ± SD	40.46 ± 1.85	1.12 ± 0.27	39.34 ± 1.79	1.41 ± 0.35	0.12 ± 0.02				
LPV	1	95.37	1.02	94.35	1.30	0.12	0.08	0.08 (0.07 - 0.10)	0.11 (0.04 - 0.19)	0.73
	2	90.07	1.29	88.78	1.20	0.13	0.08			
	3	75.63	1.64	73.99	1.20	0.13	0.09			
	4	76.57	1.30	75.27	0.99	0.16	0.08			
	Mean ± SD	84.41 ± 9.84	1.31 ± 0.25	83.1 ± 10.05	1.17 ± 0.13	0.14 ± 0.02				

ER: efflux ratio; TRQ: tariquidar; $ER_{P\text{-}gp}$: transporter-mediated component of ER; LP: total protein in MDCK cell lysate; REF: relative expression factor (measured by targeted proteomics); Predicted $K_{p,uu}$: value predicted using the ER-REF (efflux ratio-relative expression factor) approach; Observed $K_{p,uu}$: value estimated from *in vivo* UV/MP ratio at term; $CI_{90\%}$: 90% confidence interval. Note: *in vivo* P-gp abundance used in REF calculations was 0.16±0.07 pmol/mg HP (mean±SD); Interexperimental variability in quantification of P-gp protein abundance in the Transwell assays was ~21%.

DMD Fast Forward. Published on August 23, 2021 as DOI: 10.1124/dmd.121.000538
This article has not been copyedited and formatted. The final version may differ from this version.

DMD Fast Forward. Published on August 23, 2021 as DOI: 10.1124/dmd.121.000538
This article has not been copyedited and formatted. The final version may differ from this version.

Figure 1.

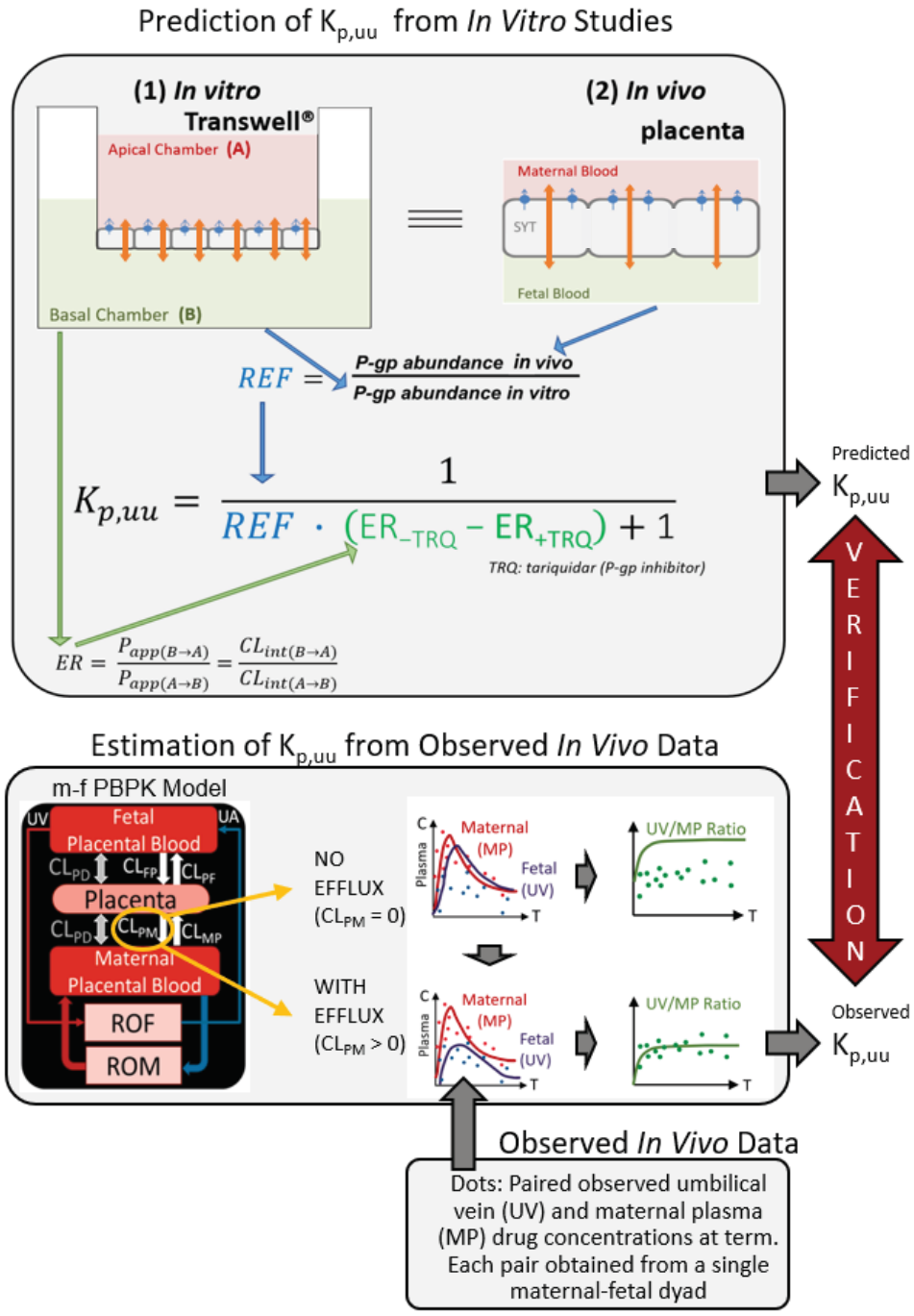

DMD Fast Forward. Published on August 23, 2021 as DOI: 10.1124/dmd.121.000538
This article has not been copyedited and formatted. The final version may differ from this version.

Figure 2.

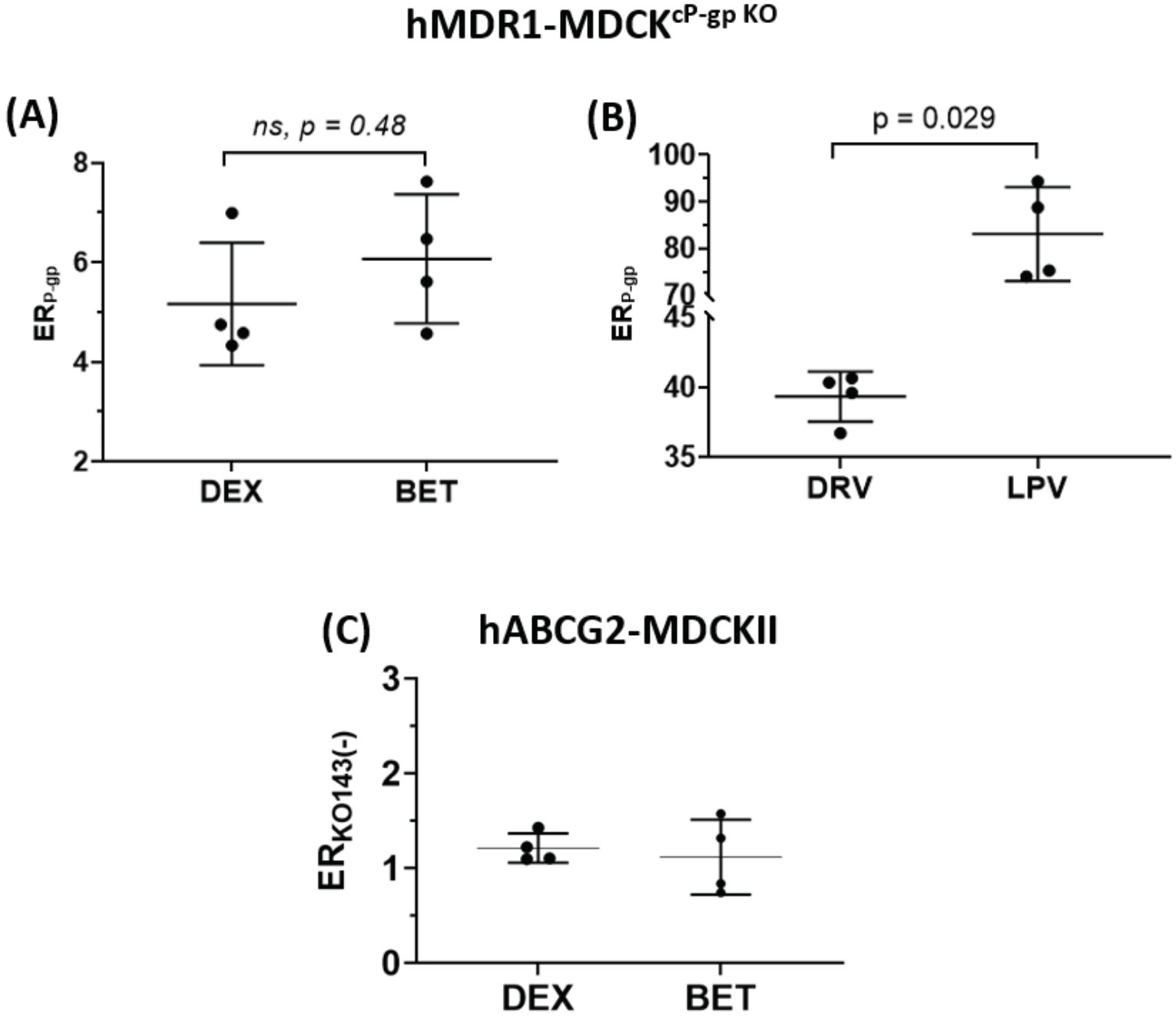

DMD Fast Forward. Published on August 23, 2021 as DOI: 10.1124/dmd.121.000538
This article has not been copyedited and formatted. The final version may differ from this version.

Figure 3.

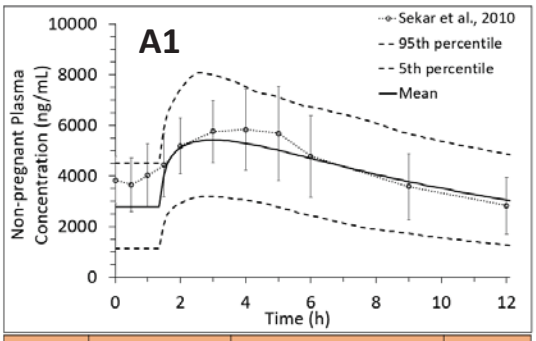

A2	Observed	Predicted (predicted / observed)	Unit
C_{max}	5821	5416 (0.93)	ng/mL
t_{max}	4	3.2 (0.8)	h
AUC_{0-12}	52601	50142 (0.95)	h*ng/mL
CL	11.4	12.0 (1.05)	L/h
AAFE	N/A	1.07	

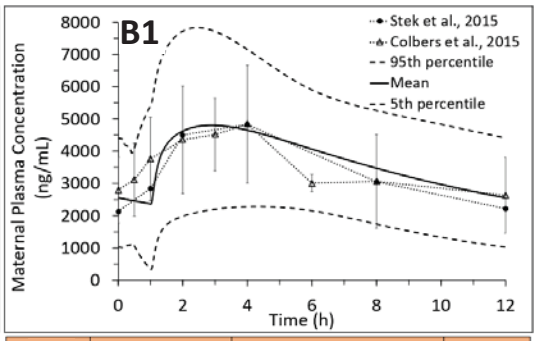

B2	Observed	Predicted (predicted / observed)	Unit
C_{max}	4830*, 4839†	4805 (0.99)	ng/mL
t_{max}	4	3 (0.75)	h
AUC_{0-12}	41818*, 41694†	44126 (1.10)	h*ng/mL
CL	14.3*, 14.4†	13.6 (0.94)	L/h
AAFE	N/A	1.15	

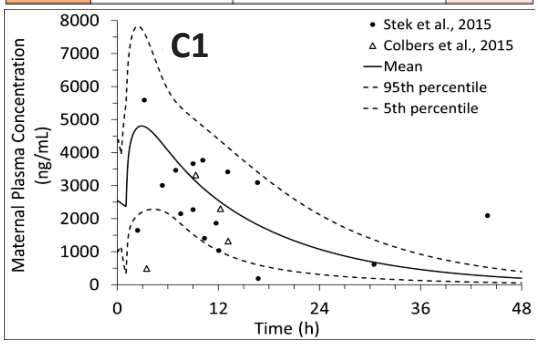

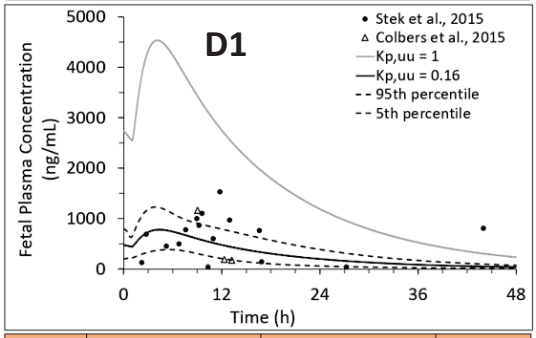

D2	Predicted $K_{p,uu}$=1	Predicted $K_{p,uu}$ = 0.16	Unit
C_{max}	4536	780	ng/mL
t_{max}	4.1	4.4	h
AUC_{0-12}	43797	7577	h*ng/mL
AAFE	6.87	2.44	

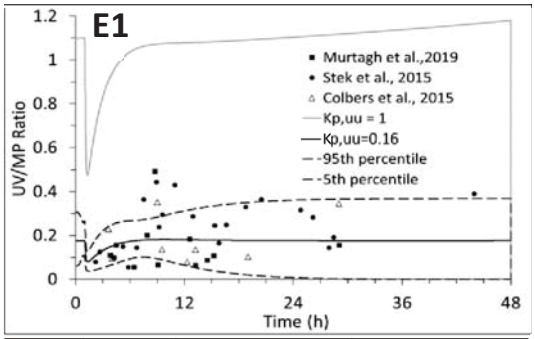

E2	Observed	Predicted $K_{p,uu}$ = 1 (predicted / observed)	Predicted $K_{p,uu}$ = 0.16 (predicted / observed)
UV/MP	0.21	1.08 (5.14)	0.17 (0.81)
AAFE	N/A	8.35	1.63

DMD Fast Forward. Published on August 23, 2021 as DOI: 10.1124/dmd.121.000538
This article has not been copyedited and formatted. The final version may differ from this version.

Figure 4.

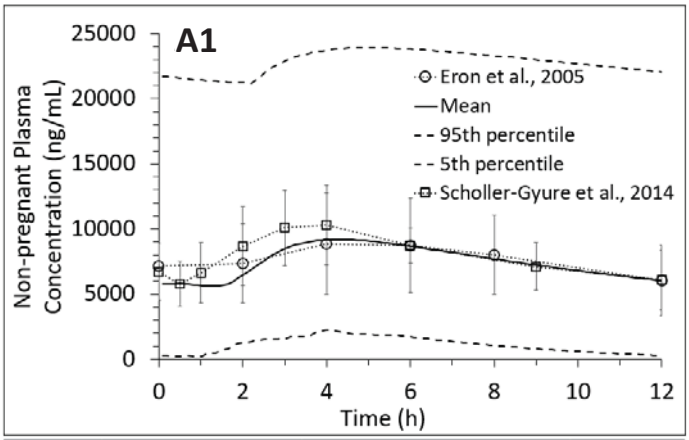

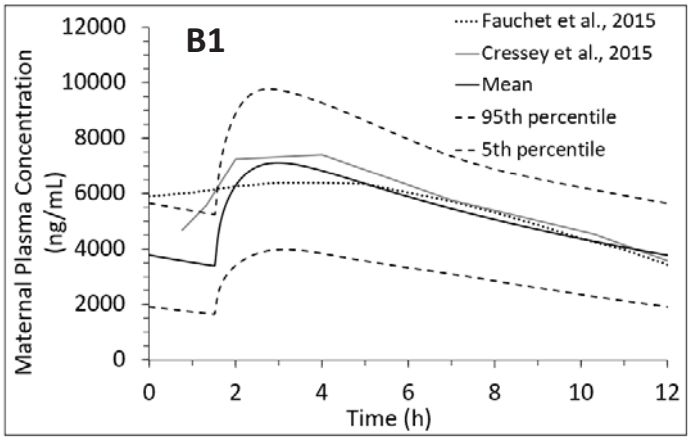

A2	Observed	Predicted (predicted / observed)	Unit
C_{max}	8885*, 10323†	8872 (0.99*,0.86†)	ng/mL
t_{max}	4	4.3 (1.07)	h
AUC_{0-12}	93333*, 96105†	90367 (0.97*, 0.94†)	h*ng/mL
CL	4.3*, 4.2†	4.4 (1.0)	L/h
AAFE	N/A	1.06*, 1.09†	

B2	PopPK Model	Predicted (predicted / observed)	Unit
C_{max}	6388*, 7409†	7064 (1.1*, 0.95†)	ng/mL
t_{max}	4	3 (0.75)	h
AUC_{0-12}	66361*, 67553†	62663 (0.94*, 0.93†)	h*ng/mL
CL	6.0*, 5.9†	6.4 (1.1)	L/h
AAFE	N/A	1.12*, 1.19†	

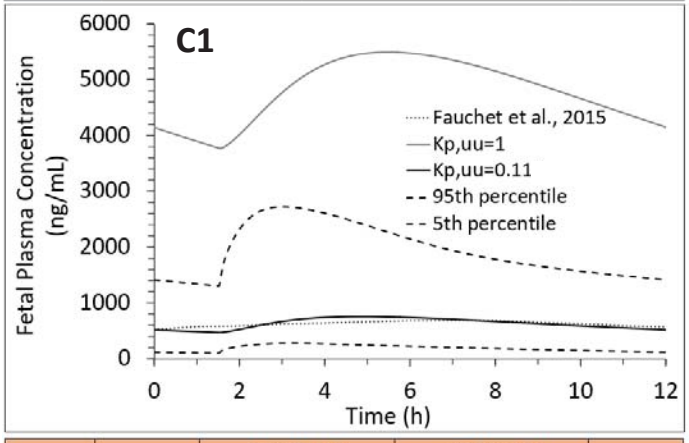

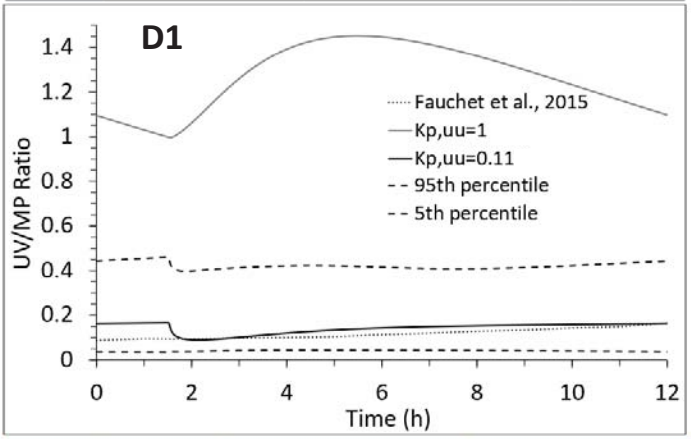

C2	PopPK Model	Predicted $K_{p,uu}$=1 (predicted / observed)	Predicted $K_{p,uu}$ = 0.11 (predicted / observed)	Unit
C_{max}	686	5494 (8.00)	756 (1.10)	ng/mL
t_{max}	7	5.48 (0.78)	4.9 (0.70)	h
AUC_{0-12}	7559	57491 (7.61)	7562 (1.00)	h*ng/mL
AAFE	N/A	7.58	1.08	

D2	PopPK Model	Predicted $K_{p,uu}$ = 1 (predicted / observed)	Predicted $K_{p,uu}$ = 0.11 (predicted / observed)
UV/MP	0.12	1.27 (10.73)	0.14 (1.20)
AAFE	N/A	6.42	1.17

DMD Fast Forward. Published on August 23, 2021 as DOI: 10.1124/dmd.121.000538
This article has not been copyedited and formatted. The final version may differ from this version.

Figure 5.

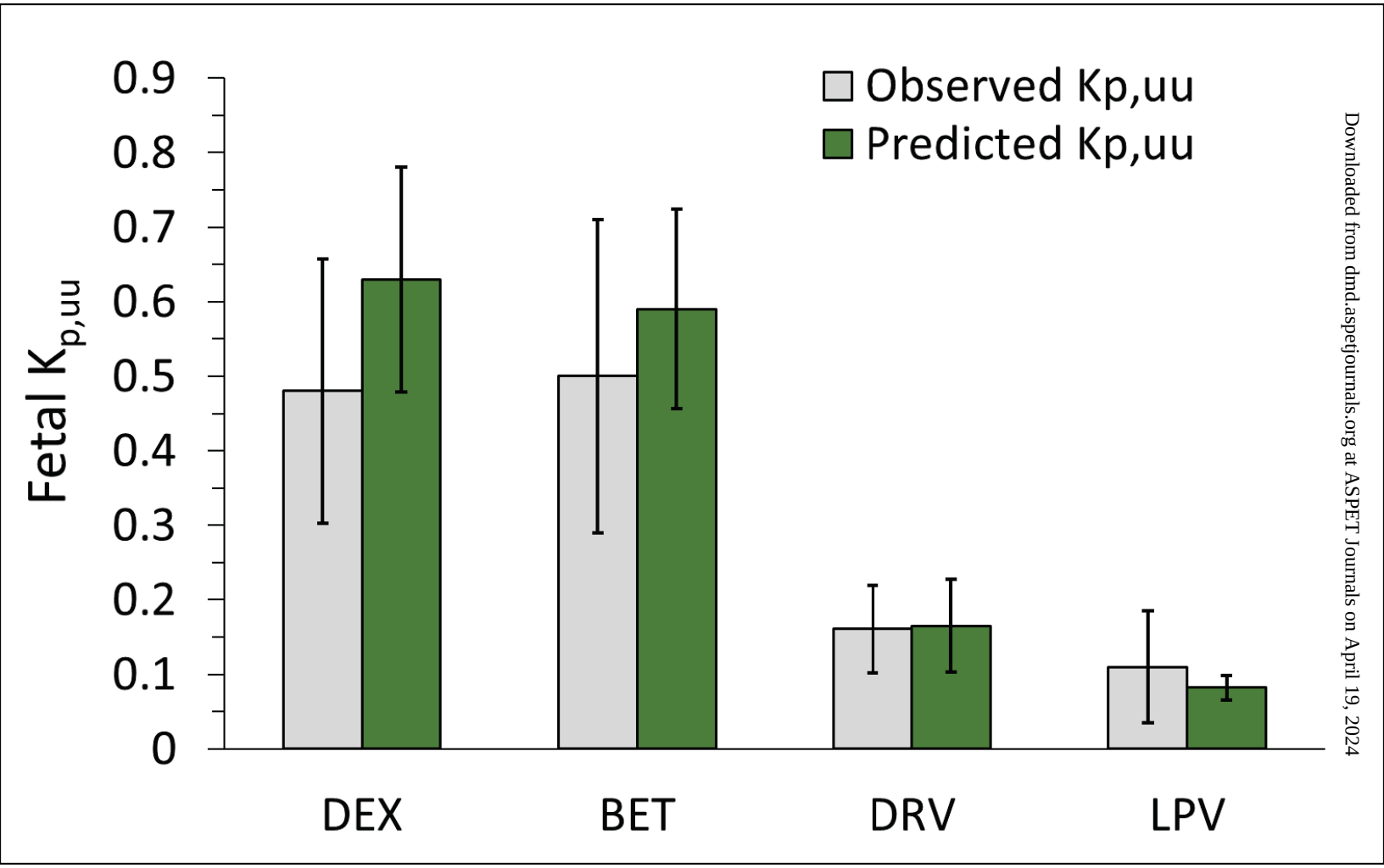

DMD Fast Forward. Published on August 23, 2021 as DOI: 10.1124/dmd.121.000538
This article has not been copyedited and formatted. The final version may differ from this version.

Figure 6.

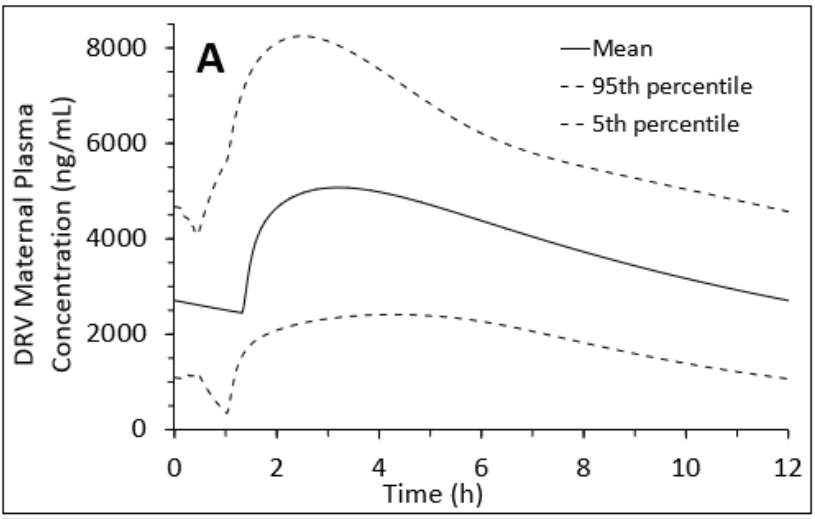

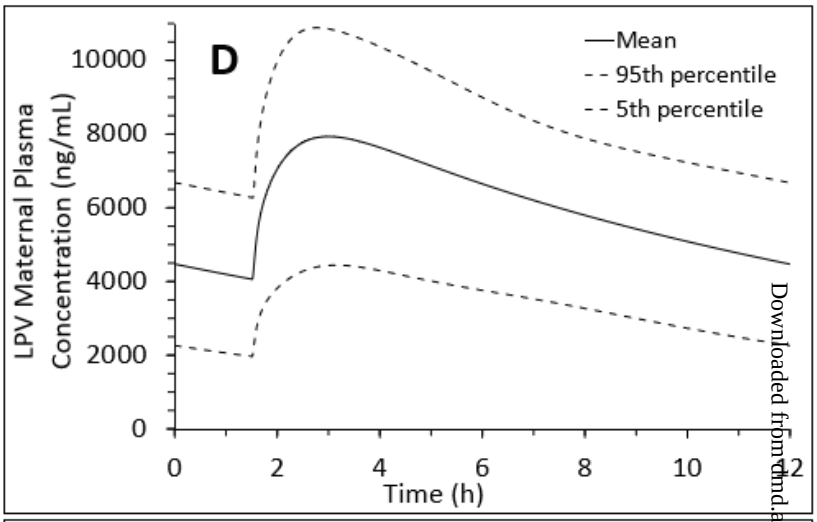

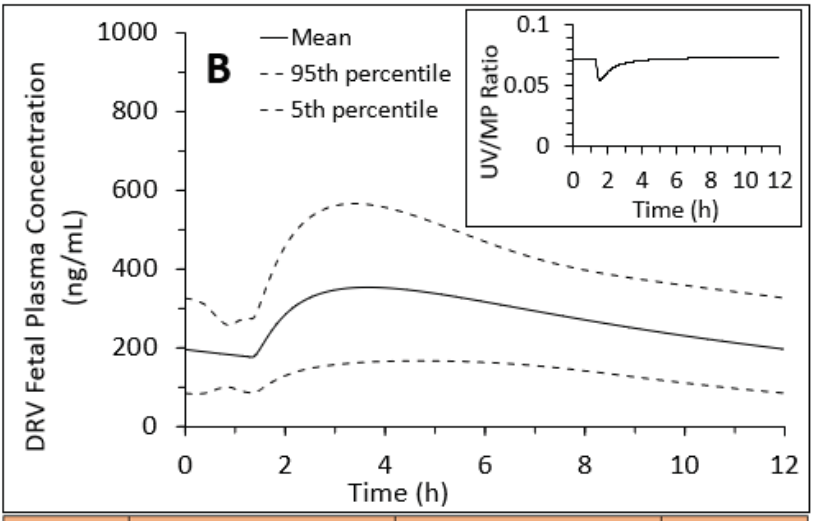

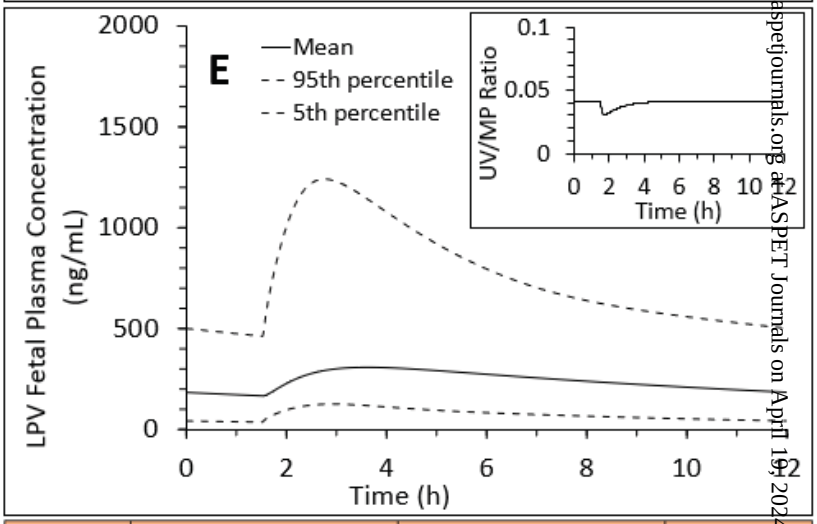

C	DRV Maternal Plasma	DRV Fetal Plasma	Unit
C_{max}	5074	353	ng/mL
t_{max}	3.2	3.6	h
AUC_{0-12}	46275	3266	h*ng/mL
UV/MP	0.07		

F	LPV Maternal Plasma	LPV Fetal Plasma	Unit
C_{max}	7935	308	ng/mL
t_{max}	3	3.6	h
AUC_{0-12}	71988	2873	h*ng/mL
UV/MP	0.04		

SUPPLEMENTARY INFORMATION

Successful Prediction of Human Fetal Exposure to P-gp Substrate Drugs Using the Proteomics-informed Relative Expression Factor Approach and PBPK Modeling and Simulation

Olena Anoshchenko, Flavia Storelli and Jashvant D. Unadkat

Department of Pharmaceutics, University of Washington, Seattle, WA

DMD-AR-2021-000538

SUPPLEMENTARY METHOD

Chemicals and Reagents

Dexamethasone (DEX), betamethasone (BET), Lucifer Yellow CH dithiothreitol (LY) were purchased from Toronto Research Chemicals (Toronto, Canada). Quinidine (QND), prazosin hydrochloride (PZS), 12 mm 0.4-µm 12-well Transwell® plates with polyester membrane inserts, 96-well white flat bottom polystyrene microplates, HEPES [4-(2-hydroxyethyl)-1-piperazineethanesulfonic acid], ProteoExtract® Subcellular Proteome Extraction Buffer II (EBII buffer), tariquidar (TRQ), Ko143, ammonium bicarbonate, sodium dodecyl sulfate (SDS) N-desmethyl loperamide, were obtained from Sigma-Aldrich (St. Louis, MO, USA). Dulbecco's Modified Eagle's medium (DMEM) with 4.5 g/L glucose (high glucose) or 1 g/L glucose (low glucose), L-glutamine and sodium pyruvate, heat-inactivated fetal bovine serum (FBS), penicillin (10,000 U/mL)–streptomycin (10,000 g/mL), 0.25% trypsin –EDTA (ethylenediaminetetraacetic acid), DPBS, Glutamax^{TM}, geneticin, Hank's balanced salt solution (HBSS) with $CaCl_2$ and $MgCl_2$, Trypan Blue, Hygromycin B (50 mg/mL), human serum albumin, iodoacetamide, acetonitrile, formic acid, methanol, chloroform was purchased from Thermo Fisher Scientific (Waltham, MA).

SUPPLEMENTARY FIGURES AND TABLES

Table S1. LC-MS/MS parameters for quantification of the compounds listed below

Compound	Parent Ion	Fragment Ions	Declustering Potential	Collision energy
Dexamethasone	393.3	373.3, 355.3	32,45	10,17
Betamethasone	393.3	373.3, 355.3	32,45	10,17
Darunavir	548.2	392.3	25	20
Quinidine	325.2	307.1, 172.0	31, 45	32, 47
Prazosin	384.2	247.2	45	40
N-desmethyl loperamide (internal standard)	463.2	252.3	71	20

Table S2. LC conditions for the compounds quantified

Column	UPLC column (ACQUITY UPLC® BEH C18 column, 1.7 µm, 2.1 mm x 50 mm, Waters)
Guard Column	C18 VanGuard Precolumn (C18, 2.1 mm x 5 mm)
Run Time	4 min
Injection Volume	5 µL
Column Oven Temperature	25°C
Autosampler Temperature	4°C

Gradient Table

Time (min)	Flow Rate (ml/min)	%A	%B
Initial	0.3	95	5
2	0.3	95	5
2	0.3	5	95
3	0.3	5	95
3.05	0.3	95	5
4	0.3	95	5

A = 0.1% formic acid in water; B = 0.1% formic acid in acetonitrile

Figure S3

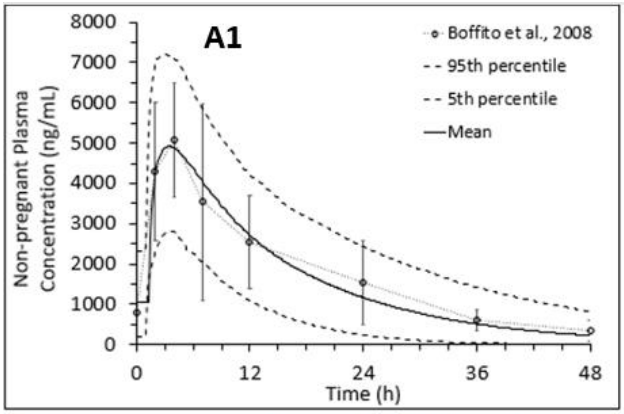

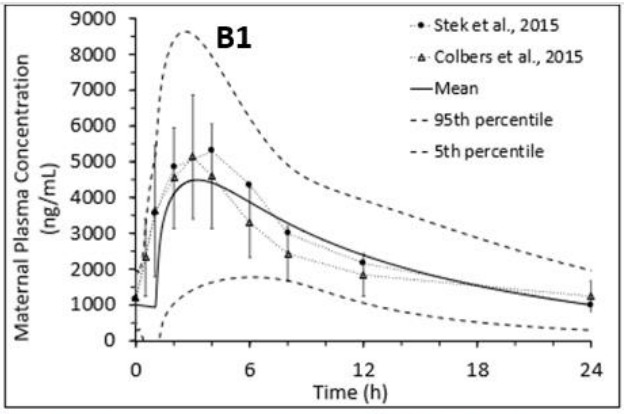

A2	Observed	Predicted (predicted / observed)	Unit
C_{max}	5079	4921 (0.97)	ng/mL
t_{max}	4	3.6 (0.9)	h
AUC_{0-24}	67007	65151 (0.97)	h*ng/mL
CL	11.9	12.3 (1.0)	L/h
AAFE	N/A	1.3	

B2	Observed	Predicted (predicted / observed)	Unit
C_{max}	5297*, 5135†	4490 (0.85*, 0.87†)	ng/mL
t_{max}	4*, 3†	3.36 (0.84*, 1.12†)	h
AUC_{0-24}	62890*, 56797†	58686 (0.93*, 1.00†)	h*ng/mL
CL	12.7*, 14.1†	13.6 (1.10*, 0.96†)	L/h
AAFE	N/A	1.38	

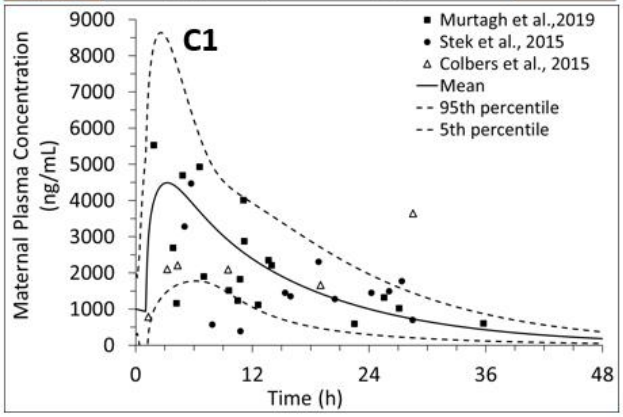

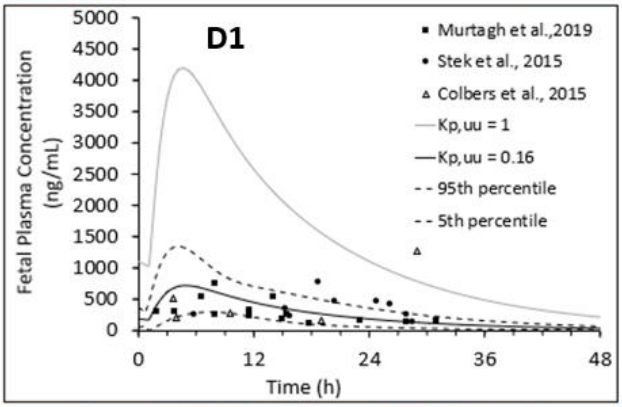

D2	Predicted $K_{p,uu}$=1	Predicted $K_{p,uu}$ = 0.16	Unit
C_{max}	4192	718	ng/mL
t_{max}	4.6	4.9	h
AUC_{0-24}	58646	10062	h*ng/mL
AAFE	6.56	1.83	

Figure S3. PBPK predictions of DRV steady-state plasma concentrations in (A1) non-pregnant individuals, (B1) pregnant women at GW34 (intensively sampled), (C1) pregnant women at GW38 (sparsely sampled) and their (D1) fetuses at GW38 (sparsely sampled) with and without incorporation of placental P-gp efflux. Subjects were administered DRV/RTV 800/100 mg PO QD. (A1) SimCYP® or **(B1, C1)** m-f PBPK predicted mean concentration-time profile (solid

line) and $Cl_{90\%}$ (dashed lines) are overlaid on the observed data (**A1**, circles: mean ± SD, n=7; **B1**, circles: mean ± SD, n=32, triangles: mean ± SD, n=17; **(C1)** sparsely-sampled observed data). **(D1, D2)** The observed fetal UV concentration-time data were better predicted by our m-f PBPK model in the presence of P-gp efflux clearance ($K_{p,uu}$ =0.16 - black solid line; dashed lines - 5th and 95th percentile profiles) vs. in the absence of P-gp efflux clearance (i.e., passive diffusion only resulting in $K_{p,uu}$=1 - grey solid line). **(A2, B2, D2)** Predicted pharmacokinetic parameters in **A2, B2** met our *a priori* defined acceptance criteria (within 0.8-1.25 fold of the observed data). The observed PK parameters were estimated from Stek *et al*., 2015 (*) or Colbers *et al*., 2015 (†).

Figure S4.

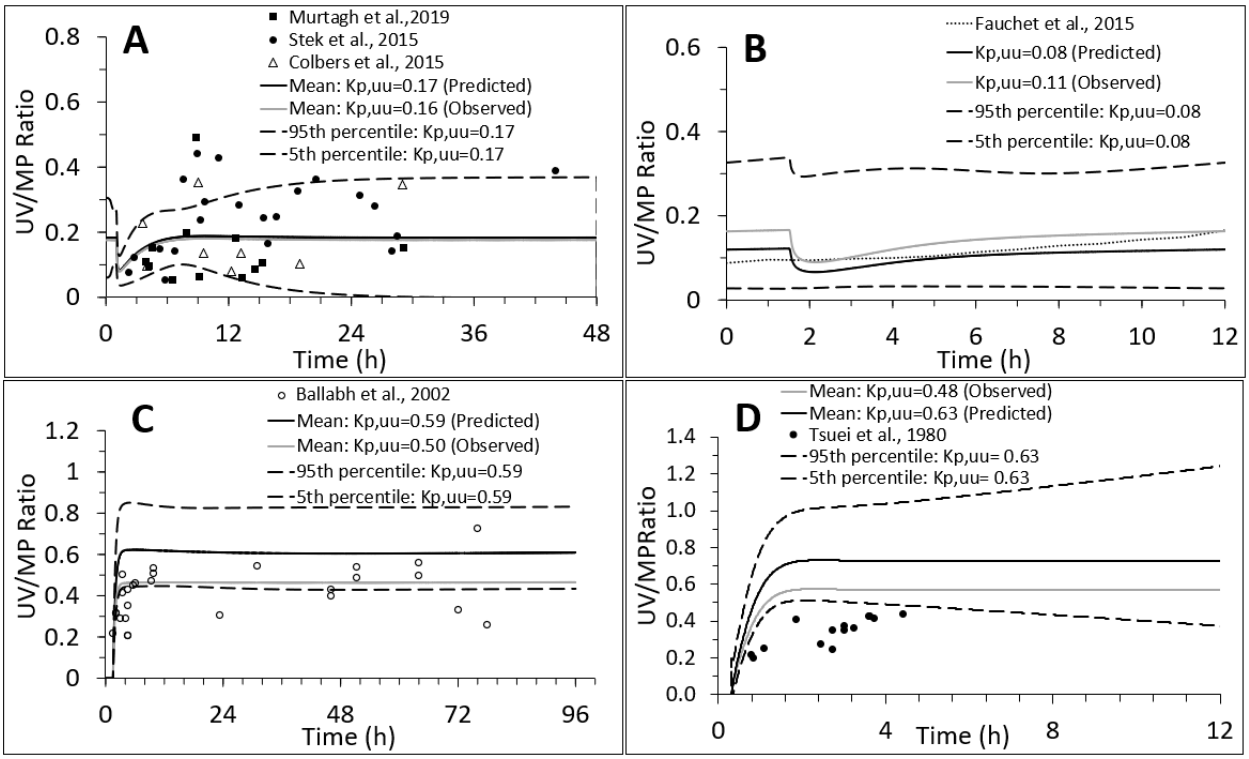

Figure S4. M-f PBPK model predictions of UV/MP ratios for (A) darunavir, (B) lopinavir, (C) betamethasone and (D) dexamethasone overlaid on the observed data (A, C, D: symbols or B: PopPK predicted – dotted line) data. Mean UV/MP ratio profile of DRV and LPV, based on ER-REF predicted $K_{p,uu}$ (black lines), are in excellent agreement with the profile based on their $K_{p,uu}$ estimated from *in vivo* studies (grey lines). In contrast, as expected from Fig. 6, the UV/MP profiles of BET and DEX, based on ER-REF $K_{p,uu,}$ modestly over-estimated the profiles generated based on their $K_{p,uu}$ estimated from *in vivo* studies. Dashed lines - 5^{th} and 95^{th} percentiles around ER-REF predicted $K_{p,uu}$ values that include variability in the virtual maternal population (See **Method**).

Table S5. Non-pregnant PBPK model input parameters for LPV, DRV and RTV

Parameter	LPV	DRV	RTV
Physico-chemical properties			
MW [g/mol]	628.81 [1]	547.7 [1]	721 [1]
Log P	4.2 [1]	2.5 [1]	3.9 [1]
Compound type	Neutral [1]	Neutral [1]	Neutral [1]
pK_a	2.6 (basic) [1] 13.4 (acidic) [1]	2.4 (basic) [1] 13.6 (acidic) [1]	2.8 (basic) [1] 13.6 (acidic) [1]
f_u	0.01 [1]	0.05 [1]	0.02 [1]
B/P	0.75 [1]	0.65 [1]	0.58 [1]
Absorption			
f_a	1 (assumed)	1 (assumed)	1 (assumed)
k_a [1/h]	0.57 (predicted) [2]	1.04 [2]	0.22 [1]
T_{lag} [h]	1.5 [2]	1.3 [2]	
Distribution			
PBPK model	Full	full [1]	minimal
V_{ss} [L/kg]	0.82 (pred) [1]	1.7 [1]	0.4 [1]
K_p scalar	0.098 [1]	1 [1]	0.048 [1]
Elimination			
CYP3A4	CL_{int}: 93.4 [1]	CL_{int}: 182 [1]	V_{max}: 1.37 [1] K_m: 0.07 [1]
CYP3A5			V_{max}: 1 [1] K_m: 0.05 [1]
CYP2D6			V_{max}: 0.7 [1] K_m: 1 [1]
CL_R [L/h]	0.15 [1]	0.3 [1]	0.27 [1]

Additional CL		Systemic: 6.5 [1] [L/h]	HLM: 50 [1] [µL/min/pmol]
Interaction - Inhibition			
CYP2B6		K_i: 500 [1]	K_i: 1.3 [1]
CYP2C9		K_i: 52 [1]	K_i: 1.22 [1]
CYP2C19		K_i: 25 [1]	
CYP2D6		K_i: 41 [1]	K_i: 0.06 [1]
CYP3A4	K_{app}: 0.41 [1] K_{inact}: 1 [1]	K_i: 0.4 [1]	K_{app}: 0.25 [1] K_{inact}: 19.8 [1]
CYP3A5	K_{app}: 1 [1] K_{inact}: 1 [1]	K_i: 0.4 [1]	K_{app}: 0.25 [1] K_{inact}: 19.8 [1]
Interaction - Induction			
CYP3A4			Ind_{max}: 68.5 [1] Ind_{C50}: 1 [1]
CYP3A5			Ind_{max}: 68.5 [1] Ind_{C50}: 2 [1]

[1] Parameters previously published in Wagner et al., 2017
[2] Parameters optimized by us in the current publication

Table S5 units:

B/P - blood:plasma partition ratio; CL_{int} - intrinsic clearance [µL/min/mg protein]; CL_R - renal clearance [L/h]; CYP - cytochrome P450; f_a - fraction absorbed; f_u - fraction of unbound drug in plasma; HLM - human liver microsomes; Ind_{C50} - inducer concentration that yields half-maximal induction [µmol/L]; Ind_{max} - inducer concentration that yields maximum induction [µmol/L]; k_a - absorption rate constant [h^{-1}]; K_{app} - concentration of mechanism-based inhibitor

associated with half-maximal inactivation rate [µmol/L]; K_i - inhibitor concentration that yields half-maximal inhibition [µmol/L]; K_{inact} - inactivation rate of given enzyme [h^{-1}]; K_m - Michaelis-Menten constant [µmol/L]; K_p - partition coefficient; log P - logarithm of octanol-water partition coefficient; MW - molecular weight [g/mol]; pK_a - negative decadal logarithm of acid dissociation constant; T_{lag} - absorption lag time [h]; pred - predicted; V_{max} - maximum rate of metabolite formation [pmol/min/mg microsomal protein]; V_{ss} - volume of distribution at steady state [L/kg]